Russian Geology and Geophysics © 2019, V.S. Sobolev IGM, Siberian Branch of the RAS
Vol. 60, No. 11, pp. 1205–1228, 2019 *DOI:10.15372/RGG2019086* *Geologiya i Geofizika*

Composition and Age of Plagiogranitoids in the South of the Lake Zone (Western Mongolia)

S.N. Rudnev[a, ✉], V.G. Mal'kovets[a,b,c], E.A. Belousova[d], I.G. Tret'yakova[a,e], A.A. Gibsher[a,b,c]

[a] *V.S. Sobolev Institute of Geology and Mineralogy, Siberian Branch of the Russian Academy of Sciences, pr. Koptyuga 3, Novosibirsk, 630090, Russia*

[b] *ALROSA Geological Research Enterprise (Public Joint-Stock Company), Chernyshevskoe shosse 16, Mirnyi, Republic of Sakha (Yakutia), 678170, Russia*

[c] *Novosibirsk State University, ul. Pirogova 2, Novosibirsk, 630090, Russia*

[d] *Australian Research Council Centre of Excellence for Core to Crust Fluid Systems/GEMOC, Department of Earth and Planetary Science, Macquarie University, Sydney, NSW 2109, Australia*

[e] *Central Research Geological Prospecting Institute of Nonferrous and Noble Metals, Varshavskoe shosse 129, korp. 1, Moscow, 117545, Russia*

Received 6 April 2018; received in revised form 1 June 2018; accepted 15 June 2018

Abstract—We consider the geologic structure, composition, and age of early Paleozoic intrusive rock associations of the Tugrug, Udzur-Hunga, Hatan-Hunga, Mandalt, Bayasgalant, and Dut Uul plutons. The plutons are located among late Neoproterozoic–early Cambrian volcanic and volcanosedimentary strata in the southern part of the island-arc system of the Lake Zone in Western Mongolia. We have recognized plagiogranitoid and gabbroid associations of different petrochemical compositions, ages, and geodynamic settings of formation in these plutons. The results of geochronological studies show that the plagiogranitoid associations in the south of the Lake Zone formed in the period from 531 to 481 Ma. Two major stages of intrusive magmatism in the zone have been established in this time interval: island-arc, 531–517 Ma, and accretion–collision, 504–481 Ma. The plagiogranitoid associations that formed at the island-arc stage are the most widespread, whereas those formed at the accretion–collision stage are much scarcer. The intrusive plutons of all ages are composed predominantly of granitoid associations of the tonalite–trondhjemite series, which are calc-alkalic rocks. Study of xenogenic and inherited zircons from plagiogranitoid associations formed at the island-arc and accretion–collision stages of the regional evolution has shown their age range 664–520 Ma. Four age groups of inherited zircon have been recognized (~664, 570–560, 545–531, and 530–520 Ma), which generally correspond to the stages of island-arc (volcanic and intrusive) and ophiolite magmatism and, most likely, reflect the additional magma-generating sources of parental plagiogranitic melts.

Keywords: granitoid magmatism, geochronology, petrochemistry, Central Asian Orogenic Belt, Lake Zone in Western Mongolia

INTRODUCTION

The Lake Zone in Western Mongolia is a late Neoproterozoic–early Cambrian island-arc terrane (Dergunov, 1989; Dergunov et al., 2001; Badarch et al., 2002), part of the Caledonian superterrane of the Central Asian Orogenic Belt (CAOB). This island-arc terrane is one of the largest in the CAOB (Fig. 1) and extends in the southern and southeastern directions for more than 800 km. In the north, the Lake Zone joins the early Caledonides of the Tannu-Ola island-arc zone of Tuva, in the west it borders upon the late Caledonides of Mongolian and Gobi Altay, and in the east, upon pre-Riphean complexes of the Dzavhan (Baydrik) microcontinent. The Lake Zone has a nappe-folded structure due to tectonically juxtaposed blocks and plates formed by late Neoproterozoic–early Cambrian fragments of ophiolite and island-arc complexes of different compositions. This belt includes a number of late Neoproterozoic stratified volcanic, volcanosedimentary, and terrigenous complexes and intruding granitoids of different ages (late Neoproterozoic–Permian) (Kutolin, 1974). Geological studies of volcanic and sedimentary complexes in different parts of the Lake Zone made it possible to establish their sizes, sequence of formation, ages (570–545 Ma), and island-arc and ophiolitic nature (Dergunov et al., 2001; Gibsher et al., 2001; Yarmolyuk et al., 2002, 2003, 2006, 2011; Kovalenko et al., 2004; Gordienko, 2006; Buriánek et al., 2017). A comprehensive study of the geologic structure and petrologic composition of volcanic and sedimentary complexes (basalt, basalt–andesite, andesite, and siliceous–terrigenous) in the northern and central parts of the Lake Zone and their petro-

✉ Corresponding author.
E-mail adress: rudnev@igm.nsc.ru (S.N. Rudnev)

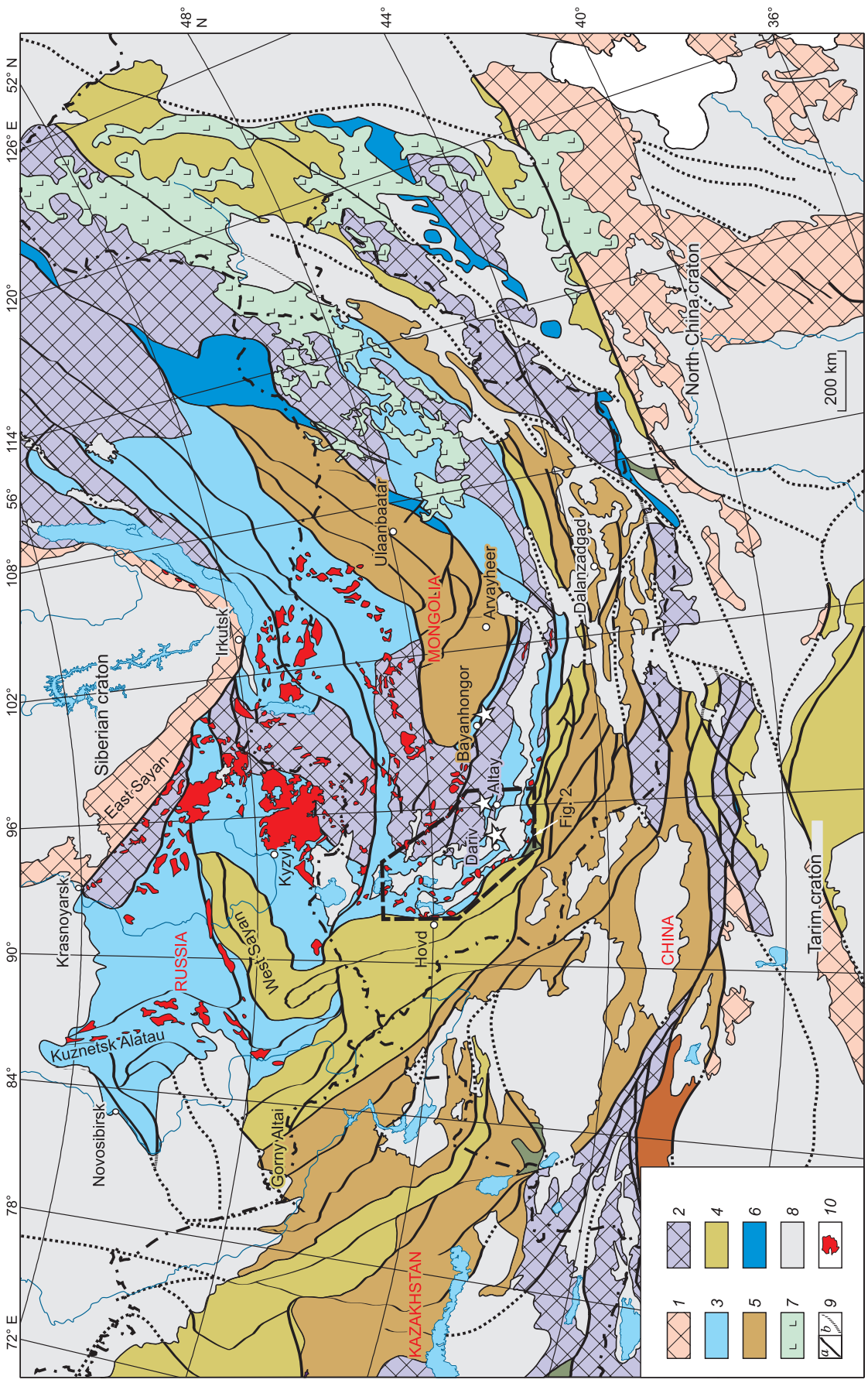

Fig. 1. Tectonic map of the Central Asian Orogenic Belt with yarly Paleozoic granitoid batholiths of the Altai–Sayan folded area and Western Mongolia, compiled after Kozlovsky et al. (2015), modified, and supplemented. Asterisk marks the position of ophiolite complexes of Western Mongolia. *1*, cratons; *2*, microcontinents; CAOB (orogenic belts): *3*, late Neoproterozoic–early Paleozoic; *4*, early–middle Paleozoic; *5*, middle–late Paleozoic, *6*, late Paleozoic–early Mesozoic; *7*, volcanic belts (late Mesozoic); *8*, Meso-Cenozoic deposits; *9*, faults: *a*, visible, *b*, predicted; *10*, early Paleozoic granitoid batholiths.

chemical, geochemical, and isotope characteristics showed that the complexes formed in different tectonic settings (oceanic plateaus and islands, island arcs, and accretionary wedges). The results of Nd isotope studies of these volcanic complexes, with regard to their geologic structure, age, and geochemical and isotope characteristics (Jahn et al., 2000a,b; Jahn, 2004; Kovalenko et al., 1996; Yarmolyuk et al., 2002, 2003, 2006, 2011, 2012; Kovach et al., 2011) led to the conclusion that the juvenile crust of the Lake Zone formed from depleted mantle sources in the intraoceanic island-arc and oceanic-plateau settings in the late Neoproterozoic–Cambrian (570–490 Ma), with involvement of ancient crustal material (sediments) in subduction zones, and during the accretion of paleo-oceanic and island-arc complexes, back-arc basins, and Precambrian Dzavhan microcontinent.

Late Neoproterozoic–early Paleozoic intrusive rock associations are widespread among island-arc volcanics of the Lake Zone, with granitoids being predominant and gabbroids being subordinate. Granitoids and gabbroids formed in different geodynamic settings (island-arc and accretion–collision) and have different ages (from late Neoproterozoic to Middle–Late Ordovician) and petrogeochemical and isotope characteristics (Izokh et al., 1998; Kovalenko et al., 2004; Rudnev et al., 2009, 2012, 2016; Yarmolyuk et al., 2011). It was established that granitoid associations in the northern and central parts of the Lake Zone, as in the Altai–Sayan folded area (Kozakov et al., 1999, 2002; Rudnev et al., 2008, 2013b, 2015; Mongush et al., 2011; Rudnev, 2013), are closely located in large polychronous batholiths (Fig. 1). In the Lake Zone, granitoid batholiths and their satellites (Rudnev et al., 2009, 2012, 2016; Yarmolyuk et al., 2011) form individual areas of intrusive magmatism (Hyargas Nuur, Har Nuur, and Bumbat Hayrhan) spaced 80–100 km apart. These areas are characterized by different structures, scales of the spread of igneous rock associations (granitoids and gabbroids), time spans of their formation, and geochemical and isotope characteristics. It was established that granitoid magmatism in these areas differed in the duration (Myr) and intensity of magmatic activity: Hyargas Nuur area—519–465, Har Nuur area—531–449, and Bumbat Hayrhan area—551–468 (Table 1). Diorite–tonalite–plagiogranite associations are predominant and granodiorite–granite associations are subordinate in the basement of large polychronous plutons in the northern and central parts of the Lake Zone. Data on the petrochemical and trace-element compositions of granitoids and their isotope characteristics are given elsewhere (Kovalenko et al., 2004; Rudnev et al., 2009, 2012, 2016; Kovach et al., 2011; Yarmolyuk et al., 2011). These data made it possible to assess the conditions of formation of the parental melts and the main magma-generating sources at different stages (island-arc and accretion–collision) of the regional geodynamic evolution.

The early Paleozoic intrusive magmatism in the south of the Lake Zone has been poorly studied. There are only a few publications (Table 1) considering the geologic structure and composition of the Tuguruk gabbroid pluton localized in the axial part of the Lake Zone island arc (Izokh et al., 1990) and the time of formation, chemical composition, and isotope characteristics of granitoid and gabbroid intrusions in the area of the Dariv, Haan Tayshiri, and Zamtyn Nuruu Ranges (Khain et al., 1995; Kozakov et al., 2002; Dijkstra et al., 2006; Jian et al., 2014; Kovalenko et al., 2014; Kröner et al., 2014; Buriánek et al., 2017; Janoušek et al., 2018).

The goal of this research work was to establish the geodynamic setting of formation of early Paleozoic granitoids in the south of the Lake Zone of Western Mongolia, the time sequence of their formation, and the likely sources of their parental melts. For this purpose, we thoroughly investigated the geologic structure of early Paleozoic granitoid plutons and the relationship of the recognized rock associations with each other and with the host rocks, performed geochronological studies of magmatic, xenogenic, and inherited zircons from the above granitoid associations, and examined the mineralogical, petrographic, and petrochemical compositions of all rock groups of the plutons. During the geochronological studies, special attention was paid to xenogenic and inherited zircons, whose U–Pb isotope studies permit estimation of the age of the rocks involved in the formation of the parental granitic melts. To solve the set goals and tasks, we studied several granitoid plutons forming individual areas of intrusive magmatism in the south of the Lake Zone. These plutons are located in the axial part of the zone island arc between the Tugrug and Darvi Samons and are an extension of the belt of early Paleozoic granitoid plutons located in the northwest within the same island-arc zone.

The conditions of generation of parental plagiogranitic melts and their magma-generating sources will be reported in our next paper, based on the study of the trace-element composition of rocks, their Sr–Nd isotope characteristics (Sm–Nd and Rb–Sr dating methods), and the Hf isotope composition of zircons.

GEOLOGIC LOCATION AND STRUCTURE OF THE PLUTONS

A number of early Paleozoic granitoid plutons are localized in the early Caledonides in the south of the Lake Zone of Western Mongolia. They form individual areas of intrusive magmatism (Tugrug, Hatan-Hunga, and Dut Uul) (Fig. 2), which differ in geologic structures, scales of the spread of intrusive rock associations, sets of rock groups (granitoids and gabbroids), and their ages and geodynamic settings of formation.

The Tugrug area of intrusive magmatism lies in the northern part of the Mongolian Altay Range (Fig. 3) and includes the Tugrug and Udzur-Hunga plutons.

The Tugrug pluton is located in the Tugrug Samon and is one of the largest intrusions (~180 km^2) in the south of the Lake Zone. Its rocks intrude late Neoproterozoic and early Cambrian island-arc volcanic and volcanosedimentary deposits and are overlain by Middle Devonian and Neogene–Quaternary deposits. The pluton has a polychronous struc-

Table 1. Results of geochronological studies of early Paleozoic granitoid associations in the Lake Zone of Western Mongolia

Intrusive area	Pluton	Association	Geochemical type	Age, Ma	Reference
Hyargas Nuur	Sharatologoy	Diorite–tonalite–plagiogranite (early phase)	High-alumina TTG	519 ± 8	(Rudnev et al., 2009)
		Diorite–tonalite–plagiogranite (late phase)	Low-alumina TTG	494 ± 10	(Rudnev et al., 2009)
	Hyargas Nuur	Diorite–tonalite–plagiogranite	High-alumina TTG	495 ± 2	(Kovalenko et al.. 2004)
	Ayrig Nuur	Granodiorite–granite	Calc-alkalic	465 ± 11	(Yarmolyuk et al., 2011)
Har Nuur	Har Nuur	Diorite	Low-alumina TTG	529 ± 6	(Rudnev et al., 2009)
		Plagiogranite	High-alumina TTG	531 ± 10	(Rudnev et al., 2009)
		Diorite–granodiorite–granite	Calc-alkalic	459 ± 10	(Rudnev et al., 2009)
	West Bayan Hayrhan	Plagiogranite	High-alumina TTG	514 ± 8	(Yarmolyuk et al., 2011)
	Bayan Hayrhan	Granodiorite–granite	Calc-alkalic	449 ± 1	(Yarmolyuk et al., 2011)
Bumbat Hayrhan	Three Hills	Diorite–tonalite–plagiogranite	High-alumina TTG	551 ± 13	(Rudnev et al., 2012, 2016)
	Hayrhan	Peridotite–pyroxenite–gabbronorite	–	511 ± 7	(Rudnev et al., 2012, 2016)
	Bumbat Hayrhan	Plagiogranite	High-alumina TTG	535 ± 6	(Rudnev et al., 2012, 2016)
		Diorite–tonalite–plagiogranite	Low-alumina TTG	524 ± 10	(Rudnev et al., 2012, 2016)
		Diorite–tonalite–plagiogranite	Low-alumina TTG	507 ± 4	(Rudnev et al., 2012, 2016)
	Gundguzin	Diorite–tonalite–plagiogranite (early phase)	High-alumina TTG	505 ± 7	(Rudnev et al., 2012, 2016)
		Diorite–tonalite–plagiogranite (late phase)	High-alumina TTG	511 ± 7	(Rudnev et al., 2012, 2016)
	Stock (Bayan Tsagaan Nuruu Range)	Plagiogranite	Low-alumina TTG	468 ± 15	(Rudnev et al., 2012, 2016)
Dut Uul	Mandalt	Diorite–tonalite–plagiogranite	High-alumina TTG	495 ± 8	(This work)
	Bayasgalant	Tonalite–plagiogranite (early phase)	High-alumina TTG	524 ± 4	(This work)
		Plagiogranite (late phase)		523 ± 2	(This work)
	Dut Uul	Plagiogranite	High-alumina TTG	481 ± 5	(This work)
Hatan-Hunga	Hatan-Hunga	Plagiogranite	High-alumina TTG	521 ± 3	(This work)
Tugrug	Tugrug	Diorite–tonalite–plagiogranite (early phase) Plagiogranite (late phase)	High-alumina TTG	530 ± 4	(Rudnev et al., 2013a)
	Udzur-Hunga	Diorite–tonalite–plagiogranite	High-alumina TTG	504 ± 3	(This work)
			High-alumina TTG	517 ± 4	(This work)
South Darvi (Dariv Range)	–	Plagiogranite	Low-alumina TTG	573 ± 6	(Kozakov et al., 2002)
		Diorite	Low-alumina TTG	515 ± 8	(Dijkstra et al., 2006)
		Granite	Calc-alkalic	498 ± 1	(Kröner et al., 2014)
		Tonalite	Low-alumina TTG	490 ± 4	(Kozakov et al., 2002)
		Plagiogranite	Low-alumina TTG	560 ± 8	(Jian et al., 2014)
		Plagiogranite	Low-alumina TTG	567 ± 4	(Jian et al., 2014)
		Microgabbro	–	568 ± 5	(Jian et al., 2014)
Haan Tayshiri (Haan Tayshiri Range)	–	Plagiogranite	Low-alumina TTG	568 ± 4	(Gibsher et al., 2001)
		Plagiogranite	Low-alumina TTG	573 ± 8	(Jian et al., 2014)
		Plagiogranite	Low-alumina TTG	566 ± 7	(Jian et al., 2014)
		Diorite	–	542 ± 4	(Buriánek et al., 2017)
		Gabbro	–	538 ± 3	(Janoušek et al., 2018)
		Gabbro	–	521 ± 6	(Janoušek et al., 2018)
		Quartz diorite	Low-alumina TTG	524 ± 7	(Janoušek et al., 2018)
		Tonalite	Low-alumina TTG	516 ± 2	(Janoušek et al., 2018)
		Quartz diorite	Low-alumina TTG	511 ± 2	(Janoušek et al., 2018)
		Diorite	Low-alumina TTG	494 ± 3	(Janoušek et al., 2018)
		Granodiorite	Calc-alkalic	495 ± 3	(Janoušek et al., 2018)

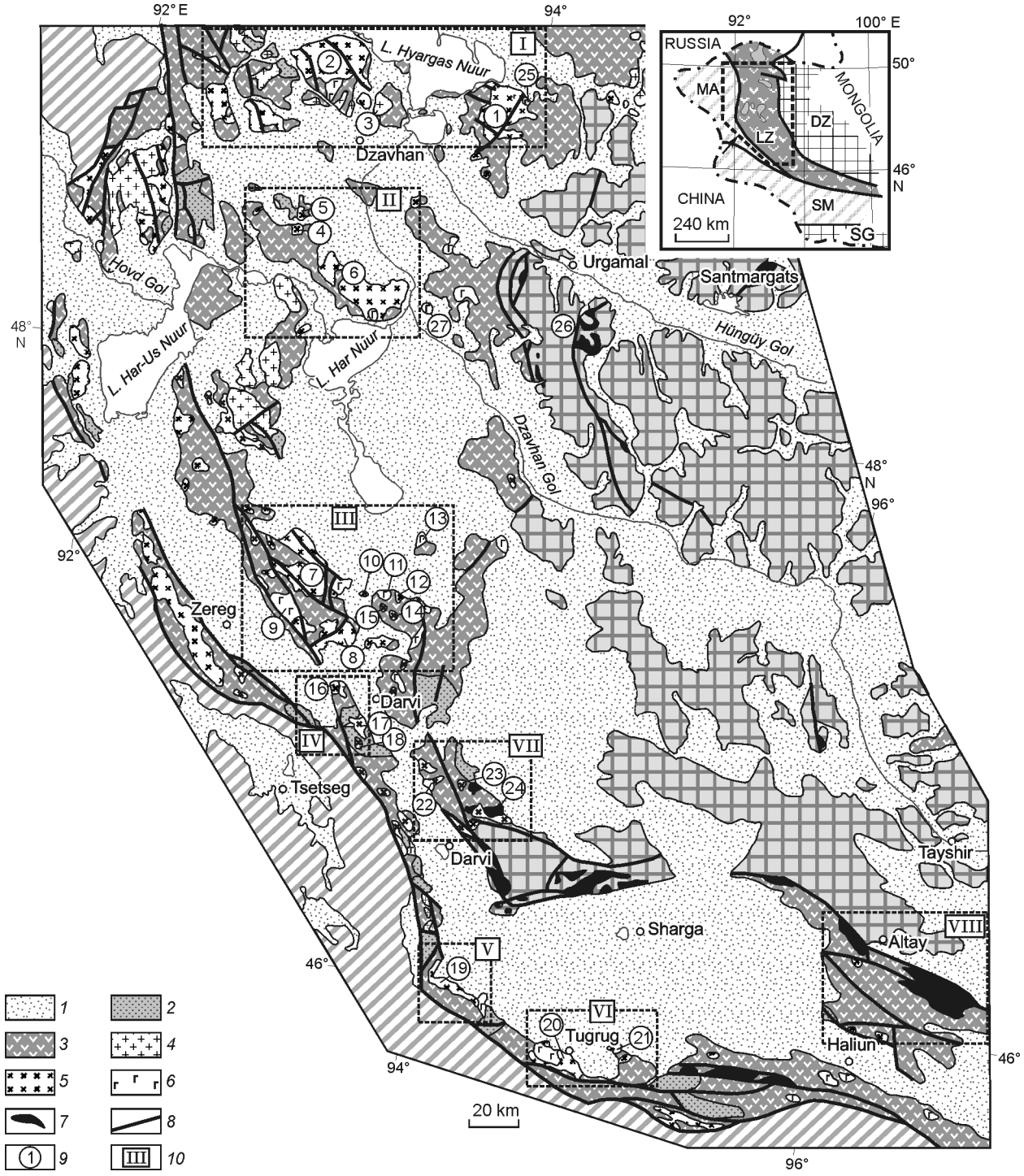

Fig. 2. Schematic geologic structure of the Lake Zone, after Tomurtogoo (1999), simplified. Plutons: 1, Sharatologoy; 2, Hyargas Nuur; 3, Ayrig Nuur; 4, Bayan Hayrhan; 5, West Bayan Hayrhan; 6, Har Nuur; 7, Gundguzin; 8, Bumbat Hayrhan; 9, Hayrhan; 10, Three Hills; 11, Bayan Tsagaan; 12, East Bayan Tsagaan; 13, Tavan Hayrhan; 14–15, Bayan Tsagaan Nuruu stock; 16, Dut Uul; 17, Bayasgalant; 18, Mandalt; 19, Hatan-Hunga; 20, Tugrug; 21, Udzur-Hunga; 22, Tungalag; 23, granitoid plutons of the Dariv Range; 24, ophiolites of the Dariv Range; 25, Hara Chulu; 26, Hutul; 27, Sar Hayrhan. Areas of intrusive magmatism: I, Hyargas Nuur; II, Har Nuur; III, Bumbat Hayrhan; IV, Dut Uul; V, Hatan-Hunga; VI, Tugrug; VII, South Darvi; VIII, Haan Tayshiri. Inset shows a schematic tectonic map of Western Mongolia. Precambrian microcontinents: DZ, Dzavhan; SG, South Gobi; LZ, Lake Zone island arc (late Neoproterozoic–early Paleozoic); accretionary complexes (early–middle Paleozoic): MA, Mongolian Altay; SM, South Mongolian. *1,* sedimentary deposits (KZ–MZ); *2*, volcanic and sedimentary deposits (S–D); *3*, volcanic and sedimentary deposits (NP_3–$Є_1$); *4*, granitoids (D); *5*, granitoids (O); *6*, gabbroids (NP_3–O_1); *7*, ophiolites (NP); *8*, faults; *9*, plutons and their numbers; *10*, intrusive areas.

ture. Gabbroids of the Hyargas Nuur complex of the Tuguruk pluton (Izokh et al., 1990) are the oldest associations, and plagiogranitoids of the Tohtogenshil complex are the youngest ones.

The Tuguruk gabbroid pluton lies in the northwest of the Tugrug pluton and occupies about 25–30% of its area. It is a typical peridotite–pyroxenite–anorthosite–gabbronorite association. The pluton has a layered structure; the layers are formed by troctolites, olivine gabbro, and plagioperidotites. Most of the rocks underwent intense amphibolization as a result of the intrusion of younger plagiogranitoids.

Geological studies showed that granitoids of the Tugrug pluton are divided into two intrusive associations with different sets of rock groups, mineral and petrographic compositions, rock structures and textures, and ages: diorite–tonalite–plagiogranite (early phase) and plagiogranite (late phase). Diabase dikes (a dike complex) are widespread within the Tugrug pluton, especially in its eastern part (Fig. 3), and in the host rocks. Geological data show two stages of the dike formation. Dikes of the early stage break through the rocks of the early diorite–tonalite–plagiogranite association and gabbroids of the Tuguruk pluton and are cut by late plagiogranites. Dikes of the late stage intrude early- and late-phase rocks and are overlain by Early Devonian volcanic and volcanosedimentary deposits.

Rocks of *early diorite–tonalite–plagiogranite association* occur in the south of the Tugrug pluton. The association comprises biotite–amphibole quartz diorites (~50%), tonalites (~40–45%), and plagiogranites (~5–10%), which form individual intrusive phases. Plagiogranite dikes form veins. They intrude earlier formed gabbroids of the Tuguruk pluton and are injected by diabase

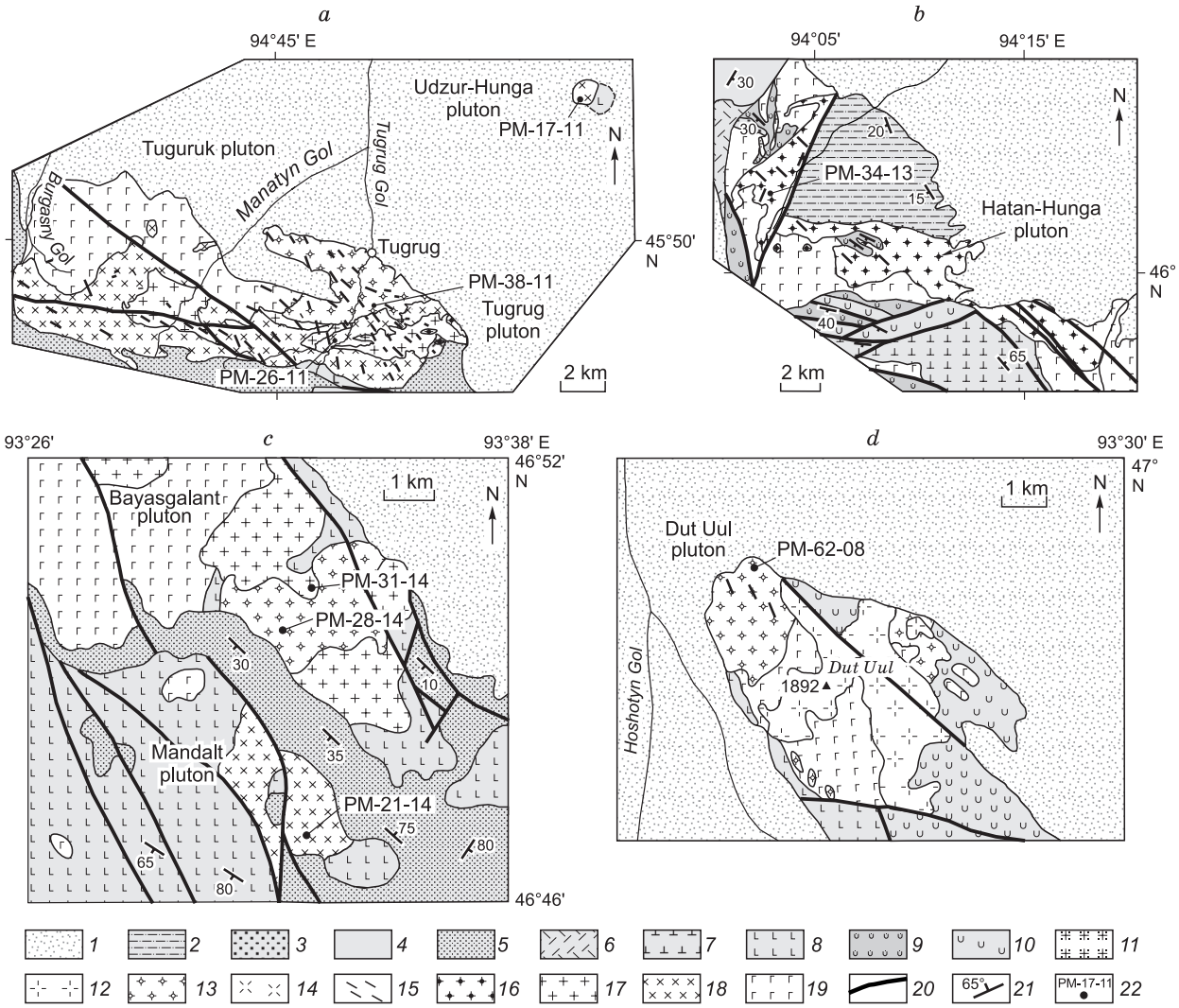

Fig. 3. Schematic geologic structure of granitoid plutons in the south of the Lake Zone, after Togtoh et al. (1993), modified and supplemented. Plutons: *a*, Tugrug and Udzur-Hunga, *b*, Hatan-Hunga, *c*, Mandalt and Bayasgalant, *d*, Dut Uul. *1*, terrigenous deposits KZ–Q; *2–5*, sedimentary and terrigenous deposits: J_1–J_2 (*2*), P_1 (*3*), C_1 (*4*), and D_2 (*5*); *6–10*, volcanic and sedimentary deposits: D_1 (*6*), $Є_1$ (*7*), V–$Є_1$ (*8*), V (*9*), and R_3–V (*10*); *11–12*, granitoids: P_2 (*11*) and C_{2-3} (*12*); *13*, tonalites and plagiogranites, $Є_3$–O_1; *14*, quartz diorites, $Є_3$–O_1; *15*, diabase dikes, $Є_3$–O_1; *16*, plagiogranites, $Є_1$; *17*, tonalites, $Є_1$; *18*, quartz diorites, $Є_1$; *19*, gabbroids, V–$Є_1$; *20*, faults; *21*, dips and strikes; *22*, sample numbers and sampling localities.

dikes and rocks of late plagiogranite association. The rocks of diorite–tonalite–plagiogranite association are coarse- to medium-grained and have a gneissoid structure.

Denuded rocks of *late plagiogranite association* occupy about 30% of the Tugrug pluton, being localized mainly in its northeastern part, where they form a large pluton within the Tugrug Samon. Less often, these rocks occur as small stock-like bodies in the north of the pluton, among the fields of early diorite–tonalite–plagiogranite association. The late association comprises equigranular coarse-grained muscovite–biotite plagiogranites with a massive structure, without signs of gneiss formation.

The Udzur-Hunga pluton lies 16 km northeast of the Tugrug pluton, near Mt. Udzur-Hunga-Nuruu (1620 m). At the present-day erosional truncation it is rounded and ~2 km^2 in area (Fig. 3*a*). Most of the pluton is overlain by Quaternary deposits; in the east they break through late Neoproterozoic–early Cambrian volcanic deposits. The pluton is composed of predominant medium- to coarse-grained gneissoid biotite–amphibole quartz diorites (60–65%) and subordinate gneissoid tonalites (25–30%) and plagiogranites (~5%). In mineral and petrographic compositions, textures, and structures the pluton rocks are similar to the rocks of early diorite–tonalite–plagiogranite association of the Tugrug pluton. There are also lamprophyre dikes and biotite–amphibole plagiogranite veins and dikes.

The Hatan–Hunga area of intrusive magmatism. This area of early Paleozoic intrusive magmatism lies in the northwest of the Tugrug area, between the Darvi (southern) and Tugrug Samons, on the northeastern flank of the Mongolian Altay Range (Fig. 2). It has an intricate structure: Gabbroid and granitoid associations break through volcanic island-arc deposits of late Neoproterozoic and early Cambrian age (Fig. 3). In the east of the area, intrusive associations border upon the middle Paleozoic Mongolian Altay deposits along a fault, and in the east and northeast they are overlain by Quaternary and Jurassic deposits. Granitoid and gabbroid associations are proximal to each other and occupy similar areas. Gabbroids occur within small intrusive plutons. They are subject to strong alteration on the flank proximal to later formed plagiogranitoids.

The Hatan-Hunga pluton is U-shaped at the present-day erosional truncation, about 50–60 km^2 in area (Fig. 3). The true size of the pluton is unclear, because the rocks in its eastern part are overlain by Quaternary and Jurassic terrigenous-sedimentary deposits. The pluton rocks break through late Neoproterozoic and early Cambrian volcanic deposits and earlier formed early Cambrian gabbroids of the Hyargas Nuur complex and are intruded by Permian granitoids. The pluton comprises massive coarse-grained muscovite–biotite plagiogranites (~60–65%) of the first phase and medium-grained leucoplagiogranites (~35–40%) of the second phase. The contacts between the rocks are sharp intrusive, with tongues of second-phase leucoplagiogranites in the first-phase plagiogranites. Veins are of limited occurrence and are mainly diabase or, seldom, plagiogranite dikes. Sometimes, there are xenoblocks of the host volcanic rocks in the endocontact zones of the pluton. In mineral and petrographic compositions, textures, and structures the pluton plagiogranitoids are similar to muscovite–biotite plagiogranites of the late association of the Tugrug pluton.

The Dut Uul area of intrusive magmatism lies on the northern margin of the Sutay Range (Fig. 2) and comprises several granitoid and gabbroid plutons localized among late Neoproterozoic–early Cambrian island-arc deposits of the Lake Zone, namely, Mandalt, Bayasgalant, and Dut Uul (Fig. 3). The plutons have different structures and sets of rock associations of different ages.

The Mandalt pluton is the southernmost in this area and is located in the bald-mountain zone at an altitude above 2700 m on the left flank of the Mandalt stow, ~20 km southwest of the Darvi Samon. The pluton is ~6 km^2 in area and has an irregular shape, stretching in the NW direction. Its rocks break through late Neoproterozoic–early Cambrian volcanic deposits and are overlain by Middle Devonian conglomerates (Fig. 3). The Mandalt pluton has a multiphase structure: phase 1—medium-grained amphibole–quartz diorites, phase 2—medium- to coarse-grained biotite–amphibole tonalites, and phase 3—fine-grained biotite–amphibole plagiogranites. Rocks of intrusive phases 1 and 2 make up the bulk of the pluton (80–90%) and are predominant in the south of the intrusion. They have a gneissoid structure and contain strongly altered and variably disintegrated xenoliths of gabbroids and the host early Cambrian volcanic deposits. Plagiogranites of phase 3 are of limited occurrence and are present as small stocks in the central and northeastern parts of the pluton and, extremely seldom, as thin veins among the rocks of phase 1 in the southern part. They also have a gneissoid structure and abound in secondary minerals (epidote and chlorite).

The Bayasgalant pluton lies ~3–4 km north of the Mandalt pluton (Fig. 3). It is oval, ~20 km^2 in area, and comprises two intrusive associations: tonalite–plagiogranite (early) and plagiogranite (late).

Rocks of the early *tonalite-plagiogranite association* occupy approximately half the pluton area. They form two bodies, in the north and in the south of the pluton, separated by rocks of the late plagiogranite association. The early intrusive association includes biotite–amphibole tonalites of phase 1 (major) and plagiogranites of phase 2. Sometimes, small xenoliths of strongly altered amphibole gabbro and quartz diorites are present. All rocks are medium-grained and have a gneissoid structure.

Intrusive rocks of the late *plagiogranite association* are widespread in the central part of the pluton, where they are best exposed on the flanks of the Bayasgalant stow. Amphibole–biotite plagiogranites of this association have a stable homogeneous massive structure, without signs of gneissosity, and are coarse-grained equigranular. Also, diabase dikes are present.

The Dut Uul pluton is located in the north of the Dut Uul area, near Mt. Dut Uul (Figs. 2 and 3). It is oval in plan,

~6 km^2 in area. The pluton granitoids break through late Neoproterozoic–early Cambrian volcanic deposits and early Cambrian gabbroids of the Hyargas Nuur complex and are intruded by early–middle Carboniferous granitoids. The Dut Uul pluton comprises medium- to coarse-grained equigranular gneissoid biotite plagiogranites. Sometimes, xenoliths of biotite–amphibole quartz diorites are present among plagiogranites. There are also veins of fine- to medium-grained porphyritic biotite plagiogranites and lamprophyre dikes.

PETROCHEMISTRY

Petrochemical description of plagiogranitoid associations of the Tugrug, Udzur-Hunga, Hatan-Hunga, Mandalt, Bayasgalant, and Dut Uul plutons in the south of the Lake Zone was made on the basis of more than 90 wet chemical analyses. Table 2 presents the results of analyses of all petrographic varieties of the studied plagiogranitoid associations.

In petrochemical characteristics the intrusive rocks of the Tugrug, Udzur-Hunga, and Dut Uul areas correspond to calc-alkalic granitoids (Fig. 4, Table 2). In the binary SiO_2–($Na_2O + K_2O$) diagrams, their composition points fall in the field of normal granitoids (Fig. 4). In the SiO_2–K_2O diagram they lie between the composition fields of low- and medium-K_2O granitoids. All rock varieties show serious domination of Na_2O over K_2O. In the A/CNK–A/NK diagram (Shand's index is 0.80–1.27), their composition points are localized in the fields of meta-aluminous and peraluminous granitoids (Fig. 4). In the triangular Ab–An–Or diagram, the studied plagiogranitoid associations fall in the composition field of rocks of the tonalite–trondhjemite series. At the earlier stages of the study of these intrusive associations, they were united into the early–middle Cambrian Tohtogenshil complex, based on their general petrochemical similarity, including their similar mineral and petrographic compositions. However, as shown below, the plagiogranitoid associations similar in petrochemical characteristics and mineral and petrographic compositions are of different ages.

U–Pb ISOTOPE STUDIES OF MAGMATIC AND XENOGENIC ZIRCONS

The Tugrug pluton. This pluton comprises two intrusive granitoid associations: diorite–tonalite–plagiogranite (early) and plagiogranite (late). To determine the age of the rocks of the diorite–tonalite–plagiogranite association, we studied the monofraction of zircon from coarse- to medium-grained gneissoid biotite–amphibole quartz diorites of the first phase (Fig. 3, sample PM-26-11) from the eastern part of the pluton. The zircons are transparent euhedral pink crystals with smooth edges and faces, a prismatic habit, and an elongation coefficient K_l (K_l is the length-to-width ratio of the crystal) equal to 1.2–3.0. The grain size of zircons varies from 150 to 500 μm. As seen from cathodoluminescence (CL) images, the zircons have coarse magmatic zoning (Fig. 5). Analyses were carried out at eight local points of magmatic zircon (Table 3). The Th/U ratios at these points vary from 0.22 to 0.69, which also indicates the magmatic nature of the zircons. The concordant age (Fig. 6) calculated over eight points is 531 ± 4 Ma (Rudnev et al., 2013a).

Magmatic zircons contain relics of "ancient" cores. Study of these cores showed that they are predominantly prismatic subeuhedral grains or, seldom, fragments of large (100–120 μm) crystals with K_l = 1.2–2.0. As seen from the CL images (Fig. 5), some grains have a distinct magmatic zoning, whereas others are dark-colored and have thin white rims, apparently indicating recrystallization. Isotope studies of six xenogenic zircon grains (Table 4, Nos. 1–6) showed younger ages in contrast to magmatic zircons overgrowing them as wide rims, which indicates a disturbance of the isotope system.

Geochronological studies of the rocks of the late *plagiogranite association* of the Tugrug pluton (Fig. 3) were carried out by examining the monofraction of zircons from massive coarse-grained muscovite–biotite plagiogranites (sample PM-38-11). The zircons are pink and light pink transparent euhedral prismatic crystals (150–200 μm; K_l = 1.5–3.5). The CL images show both magmatic and xenogenic zircons. Magmatic zircons have a distinct thin oscillatory zoning. Analyses of eight magmatic-zircon crystals (Table 3) showed Th/U = 0.24–0.87. The concordant age estimated over these crystals is 504 ± 3 Ma (MSWD = 0.15) (Fig. 6).

Relics of "ancient" zircon cores are detected in the central zones of the above magmatic zircons. They are present as round and prismatic grains 50 to 100 μm in size (K_l = 1.5–3.0). Their CL image (Fig. 5) shows magmatic zoning and thin white rims, apparently reflective of recrystallization processes. Some grains that are dark in the CL image are not zoned. Analytical studies were carried out for six grains of xenogenic zircon (Table 4, Nos. 9–12). The isotope ratios in these grains point to a disturbance of the isotope system. Concordant age has been established for only two zircon grains (Table 4, Nos. 7 and 8; Fig. 6). The CL images show that one of these grains is a fragment of a large crystal with clear signs of rounding and fine magmatic zoning (Fig. 5). This grain is characterized by Th/U = 0.43, and its concordant age is 563 ± 6 Ma (Table 4, Fig. 6). Note that this inherited zircon grain has a wide rim of newly formed magmatic zircon reflecting the age of crystallization of the plagiogranitic melt (504 ± 3 Ma, see above). Therefore, we assume that sedimentary rocks (resulted from supplied disintegrated igneous rocks) containing zircons with such morphological characteristics and age stayed in the melt for a long time and were contaminated with it (probably, at the magma generation depth). Hence, rocks of this age can be considered an additional source of matter during the generation of the parental melt.

As seen from the CL images, the second grain of inherited zircon is a fragment of a small prismatic subeuhedral

Table 2. Contents of major components in representative samples of plagiogranitoid plutons in the south of the Lake Zone of Western Mongolia

Component	Tugrug pluton Diorite–tonalite–plagiogranite association (early phase)								Tugrug pluton Plagiogranite association (late phase)			
	PM-31-11	PM-30-11	PM-26-11	PM-24-11	PM-20-11	PM-19-13	PM-20-13	PM-7-13	PM-37-11	PM-24-13	PM-40-11	PM-38-11
SiO_2, wt.%	57.77	60.45	62.31	63.25	63.81	64.28	67.82	71.15	71.21	71.56	71.88	72.58
TiO_2	0.45	0.44	0.40	0.44	0.43	0.43	0.20	0.27	0.03	0.02	0.03	0.03
Al_2O_3	19.10	19.20	18.35	18.70	17.80	17.22	17.80	15.04	16.70	15.33	16.05	15.95
$Fe_2O_{3\ tot}$	6.28	5.39	4.93	4.22	4.40	4.71	2.40	2.63	2.34	2.55	1.75	2.15
MnO	0.10	0.08	0.08	0.07	0.09	0.09	0.03	0.07	0.06	0.06	0.03	0.06
MgO	2.86	2.14	1.74	1.49	2.02	1.75	0.62	0.86	0.45	0.49	0.49	0.45
CaO	6.53	5.65	5.13	5.04	5.20	5.06	4.53	2.66	1.70	2.37	1.74	1.30
Na_2O	4.71	4.77	4.98	5.28	4.43	4.65	5.04	4.54	5.47	5.19	5.99	5.37
K_2O	1.15	1.05	1.05	0.74	1.42	1.26	1.06	1.87	1.42	1.28	0.73	1.36
LOI	1.21	0.89	0.69	0.82	0.86	0.57	0.95	0.53	0.75	0.60	0.95	0.81
P_2O_5	0.21	0.21	0.20	0.17	0.14	0.19	0.12	0.09	0.05	0.05	0.03	0.04
Total	100.37	100.27	99.86	100.22	100.60	100.20	100.58	99.70	100.18	99.50	99.67	100.10

Table 2 (*continued*)

Component	Udzur-Hunga pluton Diorite–tonalite–plagiogranite association				Hatan-Hunga pluton Plagiogranite association			Mandalt pluton Diorite–tonalite–plagiogranite association			
	PM-18-11	PM-16-11	PM-19-15	PM-19/1-11	PM-37-13	PM-36-13	PM-34-13	PM-26-14	PM-25-14	PM-21-14	PM-23-14
SiO_2, wt.%	57.53	60.21	62.58	74.88	71.82	72.40	73.70	58.05	59.29	64.68	67.20
TiO_2	0.50	0.55	0.42	0.08	0.13	0.10	0.10	0.66	0.57	0.31	0.41
Al_2O_3	19.25	18.60	17.27	14.20	15.87	15.47	15.32	17.42	17.13	17.40	16.14
$Fe_2O_{3\ tot}$	6.47	6.00	5.62	2.14	1.93	1.89	1.69	5.81	5.57	4.41	2.92
MnO	0.13	0.10	0.10	0.02	0.07	0.06	0.07	0.08	0.08	0.05	0.03
MgO	3.28	2.64	2.27	0.23	0.37	0.31	0.37	3.48	3.80	1.46	1.60
CaO	7.10	6.31	5.43	3.09	2.42	2.19	1.81	5.94	5.72	3.66	3.87
Na_2O	4.16	4.32	4.17	4.21	5.37	5.51	5.59	4.72	4.72	5.02	4.69
K_2O	0.83	0.90	0.89	0.37	1.22	0.96	1.03	1.28	0.97	1.49	0.86
LOI	1.25	0.80	1.07	0.41	0.92	0.59	0.87	2.15	1.27	1.04	1.50
P_2O_5	0.16	0.16	0.13	0.02	0.06	0.07	0.05	0.22	0.20	0.11	0.13
Total	100.66	100.59	99.96	99.65	100.16	99.55	100.61	99.81	99.30	99.63	99.34

Table 2 (*continued*)

Component	Bayasgalant pluton								Dut Uul pluton				
	Tonalite–plagiogranite association (early phase)					Plagiogranite association (late phase)			Plagiogranite association				
	PM-38-14	PM-35-14	PM-30/2-14	PM-30-14	PM-31-14	PM-28-14	PM-29-14	PM-33-14	PM-10-11	PM-13-11	PM-4-11	PM-63-08	PM-62-08
SiO_2, wt.%	66.31	67.95	70.14	72.17	73.05	71.50	72.33	72.54	68.60	71.36	71.78	71.27	71.27
TiO_2	0.47	0.44	0.34	0.33	0.31	0.30	0.29	0.23	0.21	0.18	0.16	0.03	0.15
Al_2O_3	15.06	14.80	14.29	13.43	13.57	13.76	13.78	13.50	18.10	16.25	16.20	15.45	15.70
$Fe_2O_{3\ tot}$	5.30	4.94	3.93	3.99	3.35	3.45	3.39	2.97	2.24	2.29	1.77	2.35	2.19
MnO	0.11	0.11	0.09	0.09	0.09	0.07	0.07	0.08	0.03	0.05	0.03	0.05	0.05
MgO	1.58	1.56	1.17	0.79	0.75	0.84	0.76	0.64	0.52	0.38	0.34	0.50	0.50
CaO	4.01	3.89	3.01	2.64	2.42	2.52	2.39	2.60	3.73	1.94	3.00	3.75	3.56
Na_2O	4.11	3.85	4.40	4.16	4.24	4.15	4.07	4.29	5.33	5.15	5.02	5.03	5.34
K_2O	1.04	1.20	1.35	1.60	1.64	1.76	1.81	1.44	0.62	1.33	1.11	0.49	0.48
LOI	1.02	0.81	1.32	0.72	0.78	0.66	0.75	0.76	0.77	1.25	0.75	0.88	0.70
P_2O_5	0.09	0.09	0.07	0.06	0.06	0.06	0.06	0.05	0.06	0.05	0.07	0.04	0.03
Total	99.11	99.64	100.09	99.98	100.27	99.09	99.71	99.09	100.21	100.23	100.23	99.84	99.97

Note. Contents of major components were determined by XRF on a SRM-25 X-ray spectrometer at the Analytical Center for Multi-Elemental and Isotope Research, SB RAS, Novosibirsk (analysts N.G. Karmanova and A.N. Toryanik).

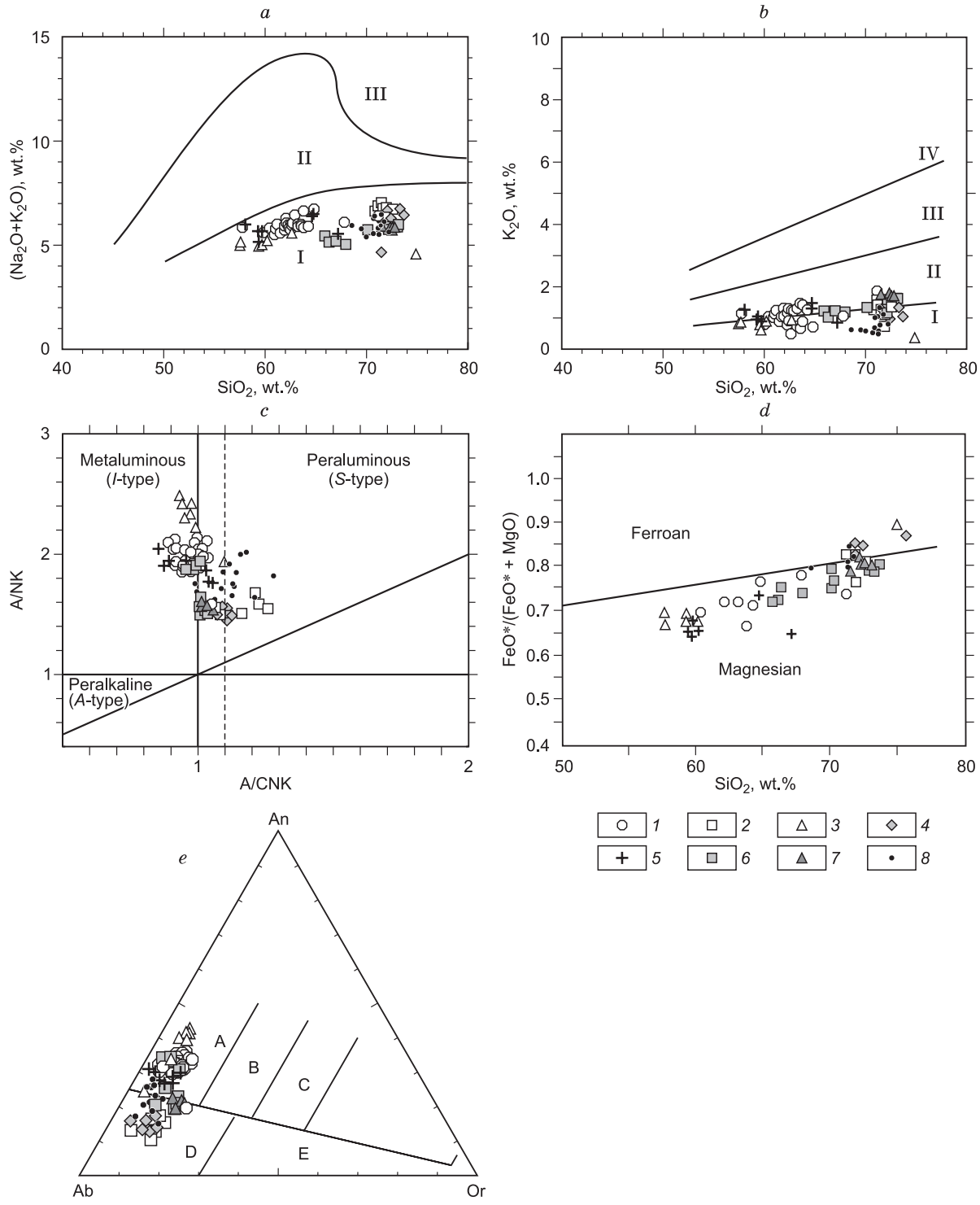

Fig. 4. Discrimination diagrams for the studied granitoid plutons: *a*, SiO_2–(K_2O + Na_2O), after Le Maitre (1989); *b*, SiO_2–K_2O, after Rickwood (1989); *c*, A/CNK–A/NK, after Maniar and Piccoli (1989); *d*, SiO_2–FeO_{tot}/(FeO_{tot} + MgO), after Frost et al. (2001); *e*, Ab–An–Or, after O'Connor (1965). A, tonalite, B, granodiorite, C, adamellite, D, trondhjemite, E, granite. Data of the rock analyses are given in Table 2. Plutons: *1*, *2*, Tugrug (early and late, respectively); *3*, Udzur-Hunga; *4*, Hatan-Hunga; *5*, Mandalt; *6*, *7*, Bayasgalant (early and late phases, respectively); *8*, Dut Uul.

crystal with smooth faces and pyramids and without magmatic zoning. It is characterized by Th/U = 0.20, which is typical of magmatic zircons. The concordant $^{206}Pb/^{238}U$ age is 524 ± 10 Ma. The wide rim (~497 Ma) on the magmatic zircon grain (~524 Ma) also indicates that the latter stayed in the plagiogranitic melt for a long time (either at the magma generation depth or during the ascent of the melt to the upper horizons of the Earth's crust). Hence, rocks of this age

Table 3. Results of U–Pb isotope studies of single zircon grains (SHRIMP-II) from plagiogranitoid plutons in the south of the Lake Zone

No.	$^{206}Pb_c$, %	U	Th	$^{232}Th/^{238}U$	$^{206}Pb^*$,	Age, Ma		$^{207}Pb^*/^{206}Pb^*$	±%	$^{207}Pb^*/^{235}U$	±%	$^{206}Pb^*/^{238}U$	±%	Rho
		ppm			ppm	$^{206}Pb/^{238}U$								
Tugrug pluton														
Diorite–tonalite–plagiogranite association, early phase, quartz diorite, sample PM-26-11														
1.1	–	68	22	0.33	5.09	539	±10	0.0588	13.1	0.707	13.2	0.087	2.0	0.15
2.1	0.80	78	23	0.30	5.58	519	±9	0.0508	14.1	0.587	14.2	0.084	1.9	0.13
3.1	0.23	155	34	0.23	11.5	534	±8	0.0533	7.5	0.636	7.6	0.086	1.5	0.20
4.1	0.59	65	40	0.63	4.81	529	±14	0.0552	27.5	0.650	27.7	0.085	2.7	0.10
5.1	0.83	111	36	0.34	8.1	525	±8	0.0523	12.3	0.612	12.5	0.085	1.7	0.13
6.1	–	55	36	0.67	4.08	531	±11	0.0691	11.1	0.818	11.3	0.086	2.1	0.19
7.1	–	53	34	0.66	3.78	511	±10	0.0683	9.7	0.777	10.0	0.083	2.1	0.21
8.1	–	52	34	0.67	3.75	515	±11	0.0710	14.2	0.814	14.4	0.083	2.3	0.16
9.1	–	73	26	0.37	5.45	539	±11	0.0639	15.3	0.768	15.4	0.087	2.1	0.14
10.1	–	40	28	0.71	3.01	536	±12	0.0638	14.1	0.762	14.3	0.087	2.4	0.17
Plagiogranite association, late phase, plagiogranite, sample PM-38-11														
1.1	0.57	56	24	0.45	3.97	512	±7.9	0.0564	7.5	0.643	7.7	0.0827	1.6	0.21
1.2	0.42	127	67	0.55	8.87	503	±6.5	0.056	3.7	0.627	4.0	0.0812	1.3	0.34
1.3	0.43	3730	3	0.01	266	512	±5.7	0.0567	1.1	0.647	1.6	0.0827	1.2	0.71
2.1	0.13	237	63	0.28	16.8	511	±6.1	0.0569	2.6	0.646	2.8	0.0824	1.2	0.43
3.1	–	264	201	0.79	18.2	497	±6.4	0.0563	2.9	0.622	3.2	0.0801	1.3	0.42
4.1	–	97	26	0.28	6.65	495	±7.4	0.0572	2.7	0.629	3.1	0.0798	1.6	0.51
5.1	0.47	309	194	0.65	21.2	494	±6.2	0.0582	1.5	0.640	2.0	0.0797	1.3	0.66
6.1	0.29	192	87	0.47	13.6	508	±6.8	0.0579	3.6	0.655	3.9	0.082	1.4	0.36
7.1	0.85	117	28	0.25	8.28	504	±8.1	0.0596	9.8	0.669	10	0.0814	1.7	0.168
8.1	0.78	100	32	0.33	6.95	497	±7.7	0.0551	7.0	0.608	7.2	0.0801	1.6	0.225
Udzur-Hunga pluton														
Diorite–tonalite–plagiogranite association, quartz diorite, sample PM-17-11														
1.1	–	168	71	0.44	12.0	516	±5.8	0.0598	2.9	0.6868	3.2	0.0833	1.2	0.37
10.1	1.71	39	9	0.25	2.9	515	±10.9	0.0534	18.5	0.6133	18.6	0.0832	2.2	0.12
2.1	1.69	41	9	0.24	3.0	524	±10.6	0.0525	18.4	0.6119	18.5	0.0846	2.1	0.11
3.1	1.35	38	7	0.20	2.7	516	±11.2	0.0572	12.7	0.6573	12.9	0.0833	2.3	0.18
4.1	0.68	79	13	0.17	5.8	521	±7.1	0.0554	7.1	0.6428	7.2	0.0842	1.4	0.20
5.1	1.14	61	19	0.33	4.4	522	±8.4	0.0547	12.0	0.6360	12.1	0.0843	1.7	0.14
6.1	0.41	190	83	0.45	13.6	513	±5.3	0.0551	6.5	0.6298	6.6	0.0829	1.1	0.16
7.1	0.55	129	36	0.28	9.3	515	±5.8	0.0581	5.8	0.6657	5.9	0.0831	1.2	0.20
8.1	0.41	198	36	0.19	14.4	520	±5.2	0.0565	4.2	0.6538	4.3	0.0840	1.0	0.24
9.1	0.94	47	11	0.25	3.4	521	±9.6	0.0560	13.4	0.6499	13.5	0.0842	1.9	0.14
Hatan-Hunga pluton														
Plagiogranite association, plagiogranite, sample PM-34-13														
1.1	0.49	100	42	0.44	7.19	517	±7.7	0.0595	5.4	0.685	5.7	0.0835	1.6	0.27
2.1	–	36	9	0.26	2.64	527	±11	0.0623	5	0.731	5.5	0.0851	2.2	0.40
3.1	0.27	179	126	0.73	13.2	531	±6.1	0.0581	3.2	0.689	3.4	0.0859	1.2	0.348
4.1	–	9	1	0.14	0.66	508	±21	0.0679	9.8	0.767	11	0.0819	4.2	0.394
5.1	3.02	18	6	0.33	1.25	495	±17	0.055	28	0.61	28	0.0798	3.5	0.12
6.1		32	6	0.21	2.24	501	±11	0.0583	5.3	0.649	5.8	0.0808	2.3	0.40
7.1	0.79	70	39	0.57	5.03	511	±8.4	0.0553	7.8	0.63	8	0.0825	1.7	0.21
8.1	0.85	191	126	0.68	14.1	528	±7.3	0.052	8.2	0.612	8.3	0.0853	1.4	0.17
9.1	–	38	8	0.21	2.8	529	±11	0.0589	4.8	0.694	5.3	0.0855	2.1	0.40
10.1	0.81	68	37	0.56	4.97	511	±8.5	0.053	8.6	0.602	8.8	0.0825	1.7	0.20

(*continued on next page*)

Table 3 (*continued*)

No.	$^{206}Pb_c$, %	U	Th	$^{232}Th/^{238}U$	$^{206}Pb^*$,	Age, Ma		$^{207}Pb^*/^{206}Pb^*$	±%	$^{207}Pb^*/^{235}U$	±%	$^{206}Pb^*/^{238}U$	±%	Rho
		ppm			ppm	$^{206}Pb/^{238}U$								
Dut Uul pluton Plagiogranite association, plagiogranite, sample PM-62-08														
1.1	0.20	355	139	0.40	24.1	488	±8.1	0.0582	2.8	0.631	3.3	0.0786	1.7	0.53
1.2	0.72	158	42	0.28	10.5	477	±9.2	0.054	7.3	0.571	7.6	0.0767	2.0	0.26
2.1	1.20	62	13	0.23	4.0	463	±11	0.0577	12	0.593	12	0.0745	2.5	0.20
3.1	0.55	128	33	0.27	8.7	492	±9.2	0.0563	6.3	0.615	6.6	0.0792	1.9	0.30
4.1	–	195	77	0.41	13.7	506	±8.3	0.0567	2.7	0.638	3.2	0.0817	1.7	0.53
4.2	0.70	139	43	0.32	9.2	475	±8.6	0.0543	7.2	0.572	7.5	0.0764	1.9	0.25
5.1	0.13	555	422	0.79	37.5	487	±7.4	0.0565	2.0	0.612	2.6	0.0785	1.6	0.62
6.1	0.81	85	26	0.31	5.8	490	±10	0.0536	9.2	0.583	9.4	0.0789	2.2	0.24
7.1	0.42	235	111	0.49	15.4	471	±7.7	0.0576	4.3	0.601	4.6	0.0758	1.7	0.37
8.1	0.38	238	95	0.41	16.0	483	±8.6	0.0565	4.2	0.606	4.6	0.0778	1.8	0.40
9.1	0.79	95	29	0.31	6.3	477	±9.6	0.0548	8.2	0.58	8.4	0.0768	2.1	0.25

Note. Pb_c and Pb*, portions of common and radiogenic lead, respectively. Correction for common lead was based on measured ^{204}Pb. Rho, correlation coefficient of the errors of determination of $^{207}Pb^*/^{235}U$ and $^{206}Pb^*/^{238}U$. The U–Pb isotope studies of single zircon grains were carried out on a SHRIMP-II ion microprobe at the Center of Isotopic Research of the A.P. Karpinsky Russian Geological Research Institute, St. Petersburg. Optical (in transmitted and reflected light) and cathodoluminescence images showing the internal structure and zoning of zircons were used to choose grain surface sites for dating. The CL images were obtained with an ABT 55 scanning electron microscope. The working distance was 25–28 mm, accelerating voltage was 20 kV, and current of the focused beam on the Faraday cup was 4–6 nA. The U/Pb isotope ratios were measured by the technique proposed by Williams (1998). The intensity of the primary beam of negatively charged molecular oxygen ions was 4 nA, and the crater diameter was 18 μm. The obtained data were processed using the SQUID program (Ludwig, 2000). The U/Pb ratios were normalized to the value of 0.0668 of the TEMORA zircon standard (Black et al., 2003). The errors of single analyses (isotope ratios and isotopic ages) are within ±1σ, and the errors of the calculated concordant ages and intercepts with the concordia are within ±2σ. Concordia plots were constructed using the ISOPLOT/EX program (Ludwig, 1999).

can also be considered an additional source of matter for the parental plagiogranitic melt.

The Udzur-Hunga pluton. To determine the age of the pluton rocks, we studied coarse-grained gneissoid biotite–amphibole quartz diorites (Fig. 3, sample PM-17-11) as the main petrographic variety. Zircon monofraction is pale pink and pink transparent well-faceted prismatic crystals (180–500 μm in size; K_l = 1.5–3.0). The CL study of the internal structure of zircon crystals (Fig. 5) showed a thin oscillatory magmatic zoning. Few crystals have xenogenic zircon in the central zone, both as elongate prismatic crystals with oval edges and faces and as angular round grains (100–150 μm). The CL images show a thin magmatic zoning in both types of xenogenic zircon. We analyzed the rims and cores of 10 crystals of magmatic zircon. The Th/U ratios in them vary in a narrow range of values, from 0.16 to 0.32 (predominantly), sometimes reaching 0.42–0.44. The concordant $^{206}Pb/^{238}U$ age estimated over 11 local points is 517 ± 4 Ma (MSWD = 0.02) (Table 3, No. 13 and Table 4; Fig. 6). Relics of more "ancient" zircon are not found in the pluton rocks.

The Hatan-Hunga pluton. Geochronological study of the age of the pluton rocks (Fig. 3) was carried out for massive coarse-grained amphibole–biotite leucoplagiogranite (sample PM-34-13). The monofraction of zircon from this rock is light pink euhedral prismatic crystals (K_l = 2–4, 150–450 μm). As seen from Fig. 5, the inner zones of the crystals have a thin oscillatory zoning typical of magmatic zircons. The results of analyses (Table 3, No. 13; Table 4; Fig. 6) of nine magmatic zircon grains show Th/U = 0.13–0.70 (on the average, 0.40) and a concordant $^{206}Pb/^{238}U$ age of 521 ± 3 Ma (MSWD = 0.06).

The central zones of the above magmatic zircons sometimes contain relics of "ancient" cores either as fragments of crystals dark and nonzoned in the CL image (Fig. 5) or as small short-prismatic subeuhedral and oval grains with weak signs of magmatic zoning. The studied grains are 50–150 μm in size, with K_l = 1.5–6.0. The analytical study shows that some of the grains have signs of disturbance of the isotope system. Concordant $^{206}Pb/^{238}U$ age values have been established for only two of the studied zircon grains: 545 ± 16 and 664 ± 18 Ma (Table 4, Nos. 14 and 15; Figs. 5 and 6); they reflect the real geochronological sequence of formation of zircons. Zircon with an age of 545 ± 16 Ma measures ~120 μm along its long axis (K_l = 2) and has a magmatic growth zoning. The Th/U ratio is 0.46, which is typical of magmatic zircons. As seen from the CL images, the zircon grain has a resorbed surface and wide rims of magmatic zircon of the late generation (~521 Ma (see above)), which suggests its long existence in the melt, i.e., it has signs of

Fig. 5. CL images of zircon grains from plagiogranitoids from the south of the Lake Zone. Circles mark the points of U–Pb isotope studies of magmatic and xenogenic/inherited zircons (Tables 3 and 4, Fig. 6). Tugrug pluton: sample PM-26-11 (quartz diorite) and sample PM-38-11 (plagiogranite); Udzur-Hunga pluton—sample PM-17-11 (quartz diorite); Hatan-Hunga pluton—sample PM-34-13 (plagiogranite); Mandalt pluton—sample PM-25-14 (quartz diorite); Bayasgalant pluton—sample PM-31-14 (plagiogranite) and sample PM-28-14 (plagiogranite); Dut Uul pluton—sample PM-62-08 (plagiogranite).

inheritance from a magmatic source during the generation of granitic melt.

The second zircon grain with an age of 664 ± 18 Ma is oval, of short-prismatic habit (70 μm; K_l = 2.5), and with a sectorial magmatic zoning. The Th/U ratio is 1.7. The grain is overgrown with magmatic zircon of the late generation (~521 Ma), corresponding to the stage of crystallization of plagiogranitic melt. This wide rim on the more "ancient" zircon indicates that the latter stayed for a long time in granitic melt (probably, at the melt generation depth), which indicates its inherited nature, as in the case of the above-described xenogenic zircon with an age of ~545 Ma. Thus, rocks with zircons with an age of ~664 Ma can also be considered additional sources of matter during the generation of parental melts for plagiogranites of the Hatan-Hunga pluton. Sedimentary rocks resulted from the destruction of igneous

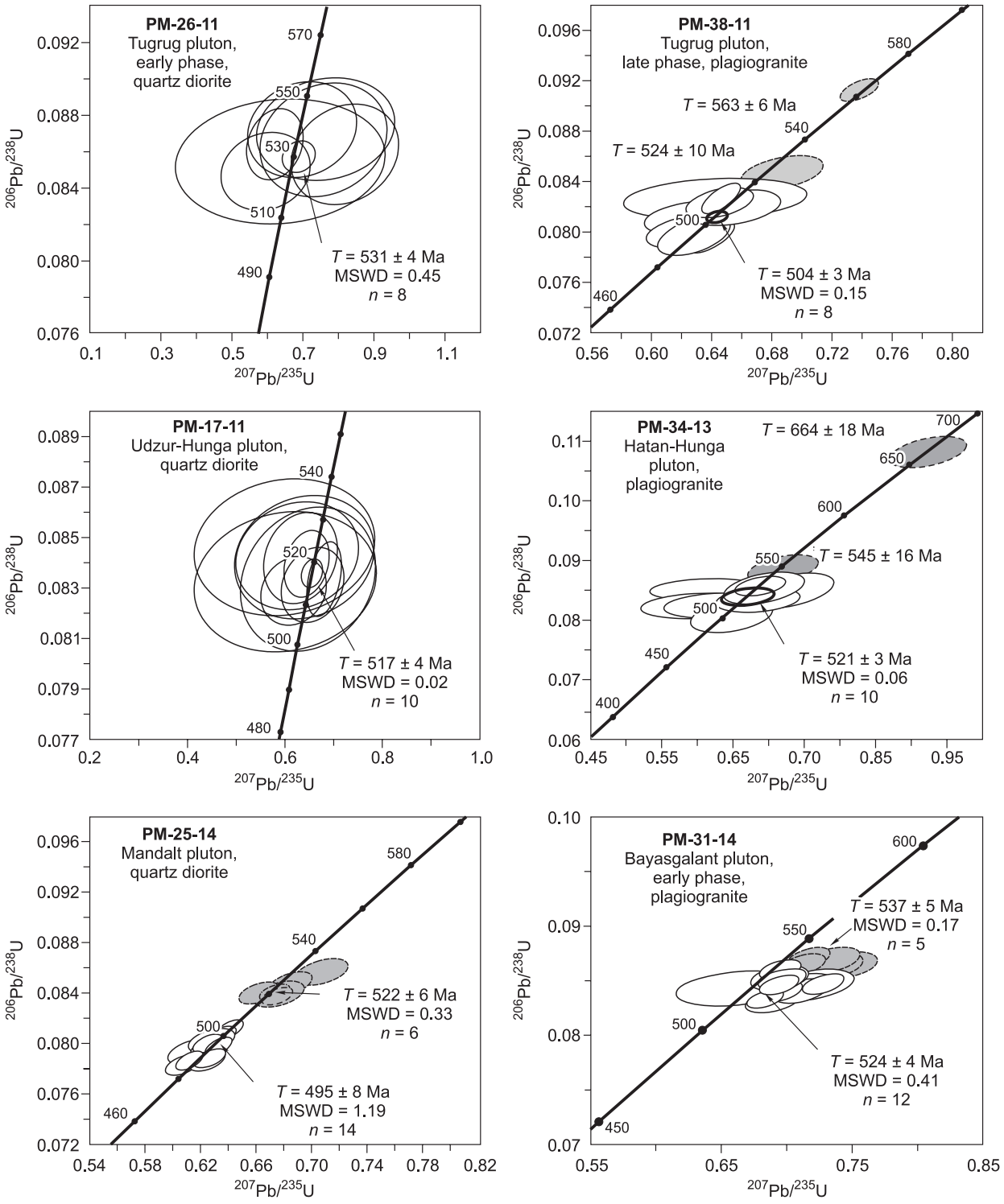

Fig. 6. Concordia diagrams for zircons from the studied plutons. Gray ellipses mark the isotope composition of xenogenic zircon.

rocks (granitoids, volcanic rocks, and their tuffs), transported into the subduction zone, and involved in melting might also have been such additional sources of matter.

The Mandalt pluton. To determine the age of the pluton rocks, we studied monofractions of zircon from medium-grained gneissoid biotite–amphibole quartz diorites (sample PM-25-14) and fine- to medium-grained biotite–amphibole tonalites (sample PM-21-14) from the southern part of the pluton (Fig. 3).

Zircons of the two monofractions are similar in morphology and have mainly euhedral transparent crystals of short- and long-prismatic habit with clear edges and faces. Subeu-

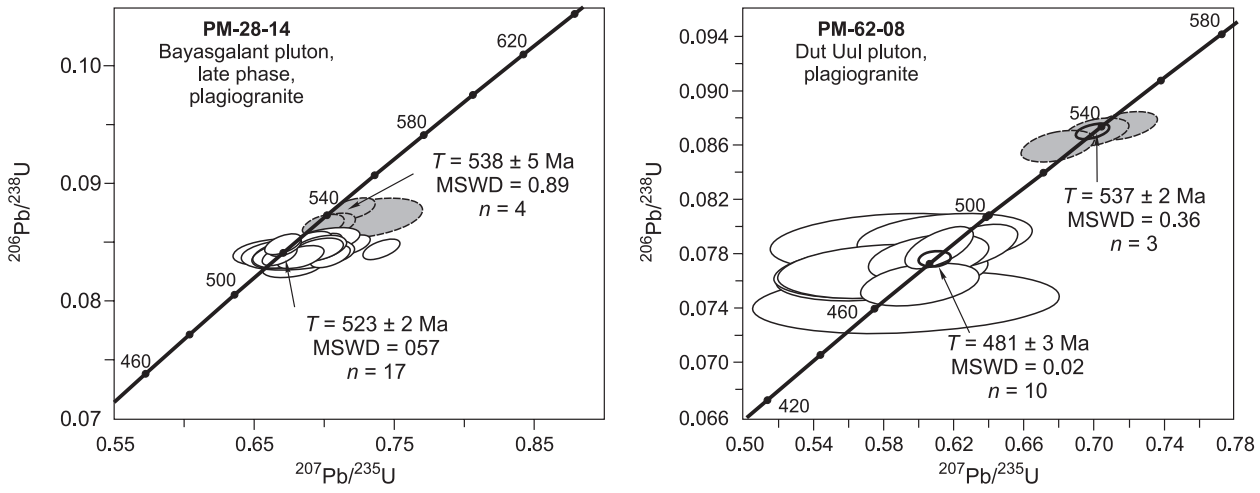

Fig. 6 (*continued*).

hedral crystals (Fig. 5) with oval edges and faces are subordinate. The crystal size varies from 30 to 200 μm (mostly 100–250 μm), K_l = 2–5 (sometimes, up to 6.5–7.0). The color of zircon varies from yellow and yellowish-pink to colorless. All zircon varieties show a magmatic zoning in CL images. Their Th/U ratio varies from 0.41 to 1.12, which also indicates their magmatic nature. Isotope studies over 14 local points of well-faceted zircon crystals (Fig. 6; Table 4, Nos. 27–40) show their concordant age of 495 ± 8 Ma (MSED = 1.19).

The central zones of the magmatic zircons contain relics of "ancient" cores. These zircons form individual grains and are, most likely, xenogenic. They are of short-prismatic habit, euhedral or subeuhedral (50–200 μm; K_l = 2–4), with magmatic sectorial and growth zoning (Fig. 6). Isotope studies over six local points of these zircons (Table 4, Nos. 47–52) showed their $^{206}Pb/^{238}U$ age of 519 to 530 Ma and their weighted average age of 522 ± 6 Ma (MSWD = 0.33). As seen from the CL images, the edges of the grains have no signs of dissolution and overgrowth with later magmatic zircon, which indicates their short-term existence in granitic melt. These zircons might have been borrowed from the host rocks approximately at the pluton formation depth. This is indicated by the presence of disintegrated xenoliths of gabbroids and volcanics on the intrusion periphery. Therefore, the host rocks cannot be considered the sources of matter during the generation of parental melts for plagiogranitoids of the Mandalt pluton.

The Bayasgalant pluton. Geochronological studies were carried out for two of its intrusive associations: tonalite–plagiogranite (early phase) and plagiogranite (late phase).

To determine the age of the *tonalite–plagiogranite association* of the early phase, we studied a monofraction of zircon from medium- to coarse-grained gneissoid biotite–amphibole plagiogranites sampled in the central part of the pluton, on the left flank of the Baysalgant stow (Fig. 3, sample PM-31-14). The monofraction is light yellow to colorless euhedral and subeuhedral transparent crystals of prismatic habit (50–150 μm in size; K_l = 2–4). In the CL image (Fig. 5), the zircons have predominantly a thin magmatic zoning. Analyses of 19 zircon grains (Table 4, Nos. 56–74) showed Th/U = 0.23–0.68. The weighted average $^{206}Pb/^{238}U$ age calculated over 12 grains of magmatic zircon (Table 4, Nos. 56–67; Fig. 6) is 524 ± 4 Ma (MSWD = 0.41).

The above magmatic zircon contains grains of inherited zircon borrowed from a magmatic source. These crystals are of prismatic habit (50–100 μm in size; K_l = 1.5–2.5), subeuhedral, with signs of slight dissolution of the edges and faces, with an internal magmatic zoning and are overgrown with zircon of the late generation corresponding to the stage of granitic-melt crystallization (~524 Ma, see above). Analyses of five grains of xenogenic zircon showed Th/U = 0.27–0.68, and the calculated $^{206}Pb/^{238}U$ age is 539–535 Ma (Table 4, Nos. 75–79; Fig. 6). The weighted average age is 537 ± 5 Ma (MSWD = 0.17).

To determine the time of crystallization of the late-phase *plagiogranite association* of the Bayasgalant pluton, we studied a monofraction of zircon from massive coarse-grained biotite plagiogranites (Fig. 3, sample PM-28-14). Zircon has light pink and yellow transparent euhedral crystals of prismatic habit (150–250 μm in size; K_l = 2–4). In the CL images they demonstrate a distinct magmatic zoning (Fig. 5). Analyses of magmatic zircons (Table 4, Nos. 80–99) showed a narrow range of Th/U ratios (0.17–0.38). The weighted average $^{206}Pb/^{238}U$ age calculated over 16 grains of magmatic zircon (Table 4, Nos. 80–95; Fig. 6) is 523 ± 2 Ma (MSWD = 0.57).

The central zone of the above magmatic zircon has relics of "ancient" zircon cores. In contrast to the xenogenic zircons from the rocks of the early-phase tonalite–plagiogranite association, these relict cores have signs of inherited zircon. As seen from the CL images (Fig. 5), they are mostly oval and slightly elongate, with signs of dissolution of the edges and faces and with a sectorial zoning typical of magmatic

Table 4. Results of U–Pb isotope study of single zircon grains (LA–ICP-MS) from plagiogranitoid plutons in the south of the Lake Zone

No.	Point	Th	U	Age, Ma, ± 2δ		Discordance, %	$^{207}Pb/^{235}U$, ± 1δ	$^{206}Pb/^{238}U$, ± 1δ	Rho
		ppm		$^{207}Pb/^{235}U$	$^{206}Pb/^{238}U$				
Tugrug pluton									
Diorite–tonalite–plagiogranite association, early phase, quartz diorite, sample PM-26-11									
1	1*	23	43	498 ± 15	510 ± 7	–15.4	0.63364 ± 0.0236	0.08237 ± 0.00114	0.37
2	2*	23	65	508 ± 12	512 ± 6	–4.1	0.64949 ± 0.02005	0.08263 ± 0.00098	0.38
3	3*	244	273	496 ± 7	497 ± 4	–1.9	0.62948 ± 0.01134	0.08023 ± 0.00066	0.46
4	4*	28	38	505 ± 17	517 ± 8	–13.8	0.64513 ± 0.02762	0.08343 ± 0.00129	0.36
5	5*	36	50	510 ± 14	510 ± 6	–0.1	0.65181 ± 0.02229	0.08229 ± 0.00107	0.38
6	6*	19	38	510 ± 25	510 ± 11	–0.4	0.65224 ± 0.04094	0.08237 ± 0.00187	0.36
Plagiogranite association, late phase, plagiogranite, sample PM-38-11									
7	4*	27	139	531 ± 22	524 ± 10	6.4	0.68704 ± 0.01780	0.08475 ± 0.0009	0.41
8	6*	145	336	561 ± 10	563 ± 6	–1.5	0.73815 ± 0.00835	0.09128 ± 0.00058	0.56
9	1*	23	104	499 ± 134	492 ± 22	7.2	0.63423 ± 0.01798	0.07933 ± 0.0009	0.40
10	2*	112	216	486 ± 180	491 ± 30	–7	0.61336 ± 0.02314	0.07919 ± 0.00112	0.37
11	3*	33	60	564 ± 224	492 ± 44	44.8	0.74310 ± 0.03712	0.07938 ± 0.00156	0.39
12	5*	481	202	844 ± 74	540 ± 22	72.2	1.29599 ± 0.02385	0.08740 ± 0.00082	0.51
Hatan-Hunga pluton									
Diorite–tonalite–plagiogranite association, quartz diorite, sample PM-34-13									
13	6	112	160	516 ± 20	526 ± 10	–11.3	0.6626 ± 0.01557	0.08499 ± 0.00083	0.42
14	1*	85	186	548 ± 34	545 ± 16	3.5	0.71614 ± 0.02839	0.0882 ± 0.00134	0.38
15	11*	122	73	665 ± 34	664 ± 18	0.8	0.92476 ± 0.0326	0.10848 ± 0.00151	0.39
16	3*	75	257	492 ± 26	516 ± 12	–35.5	0.62406 ± 0.0202	0.08332 ± 0.00104	0.39
17	4*	1672	2094	476 ± 12	435 ± 6	37.1	0.59847 ± 0.00911	0.06987 ± 0.00053	0.50
18	5*	5	26	486 ± 68	497 ± 30	–13.6	0.61466 ± 0.05376	0.08009 ± 0.00245	0.35
19	7*	108	193	516 ± 44	494 ± 20	20.8	0.66264 ± 0.03679	0.07967 ± 0.00164	0.37
20	8*	44	149	509 ± 28	507 ± 14	2.4	0.65134 ± 0.02328	0.08186 ± 0.00113	0.39
21	9*	87	146	504 ± 18	504 ± 10	0.2	0.64229 ± 0.01505	0.08126 ± 0.00079	0.41
22	10*	30	103	517 ± 22	513 ± 10	4	0.66361 ± 0.0174	0.08286 ± 0.00088	0.41
23	12*	16	74	480 ± 26	498 ± 12	0.8	0.60445 ± 0.02022	0.08026 ± 0.001	0.37
24	13*	264	787	448 ± 18	434 ± 8	17.2	0.55516 ± 0.01391	0.06971 ± 0.00072	0.41
25	14*	162	222	468 ± 74	467 ± 12	67	0.58599 ± 0.05803	0.07506 ± 0.00108	0.15
26	15*	344	435	677 ± 42	355 ± 8	86.7	0.94764 ± 0.03993	0.05663 ± 0.00063	0.26
Mandalt pluton									
Diorite–tonalite–plagiogranite association, quartz diorite, sample PM-25-14									
27	6	528	650	493 ± 8	496 ± 6	–3.7	0.62574 ± 0.00700	0.08006 ± 0.00050	0.56
28	9	1000	946	498 ± 8	495 ± 6	3.1	0.63332 ± 0.00636	0.07988 ± 0.00048	0.60
29	10	807	898	493 ± 10	495 ± 6	–1.9	0.62524 ± 0.00784	0.07977 ± 0.00054	0.54
30	20	549	708	495 ± 14	498 ± 8	–3.5	0.62835 ± 0.01093	0.08032 ± 0.00065	0.47
31	29	1169	1060	484 ± 8	489 ± 6	–6.5	0.61064 ± 0.00621	0.07882 ± 0.00049	0.61
32	30	417	499	482 ± 10	486 ± 6	–5.9	0.60725 ± 0.00794	0.07837 ± 0.00052	0.51
33	44	390	511	494 ± 10	490 ± 6	5.2	0.62693 ± 0.00743	0.07893 ± 0.00051	0.55
34	47C	368	507	493 ± 10	489 ± 6	5.4	0.62532 ± 0.00844	0.07874 ± 0.00055	0.52
35	47R	435	602	485 ± 12	493 ± 8	–10.1	0.61218 ± 0.01006	0.07944 ± 0.00061	0.47
36	2	239	318	508 ± 8	506 ± 6	2.4	0.64937 ± 0.00727	0.08163 ± 0.00051	0.56
37	23C	366	549	497 ± 10	504 ± 6	–8	0.63187 ± 0.00767	0.08128 ± 0.00054	0.55
38	34	288	415	509 ± 10	507 ± 6	2	0.65102 ± 0.00746	0.08188 ± 0.00052	0.55
39	27	575	515	479 ± 12	481 ± 6	–3	0.60272 ± 0.00972	0.07751 ± 0.00057	0.46

(*continued on next page*)

Table 4 (*continued*)

No.	Point	Th	U	Age, Ma, ± 2δ		Discordance, %	$^{207}Pb/^{235}U$, ± 1δ	$^{206}Pb/^{238}U$, ± 1δ	Rho
		ppm		$^{207}Pb/^{235}U$	$^{206}Pb/^{238}U$				
Mandalt pluton									
Diorite–tonalite–plagiogranite association, quartz diorite, sample PM-25-14									
40	32	325	512	514 ± 12	505 ± 6	9.4	0.65907 ± 0.00907	0.08149 ± 0.00057	0.51
41	13	593	614	502 ± 12	488 ± 6	14.6	0.63903 ± 0.00982	0.07856 ± 0.00056	0.46
42	4	129	229	514 ± 14	484 ± 8	26.6	0.65967 ± 0.01211	0.07803 ± 0.00066	0.46
43	33	704	788	488 ± 10	477 ± 6	11.5	0.61641 ± 0.00738	0.07687 ± 0.00057	0.55
44	37	441	602	531 ± 10	493 ± 6	30.6	0.68775 ± 0.00846	0.07952 ± 0.00053	0.54
45	21	606	680	597 ± 48	481 ± 8	71	0.8003 ± 0.04214	0.07743 ± 0.00073	0.18
46	41	128	311	497 ± 4	487 ± 8	10.5	0.63143 ± 0.01178	0.07853 ± 0.00065	0.44
47	3*	50	185	523 ± 10	520 ± 6	2.8	0.67377 ± 0.00877	0.08407 ± 0.00056	0.51
48	7*	71	211	524 ± 10	519 ± 6	5.2	0.67498 ± 0.00900	0.08378 ± 0.00057	0.51
49	14*	40	170	543 ± 14	530 ± 8	11.6	0.70662 ± 0.01233	0.08571 ± 0.00069	0.46
50	28C*	41	177	529 ± 12	525 ± 8	5.0	0.68428 ± 0.01030	0.08478 ± 0.00062	0.49
51	28R*	39	183	516 ± 12	520 ± 6	–5.2	0.66166 ± 0.00915	0.08406 ± 0.00058	0.50
52	40*	110	196	525 ± 14	520 ± 8	4.9	0.67632 ± 0.01179	0.08397 ± 0.00066	0.45
53	1*	807	942	518 ± 8	514 ± 6	3.9	0.66554 ± 0.00597	0.08305 ± 0.00048	0.64
54	15*	1297	1741	516 ± 16	512 ± 8	5.2	0.66209 ± 0.01346	0.08258 ± 0.00074	0.44
55	25*	64	225	527 ± 12	513 ± 8	13.7	0.68054 ± 0.00976	0.08278 ± 0.00059	0.50
Bayasgalant pluton									
Tonalite–plagiogranite association, early phase, tonalite, sample PM-31-14									
56	1	29	97	538 ± 16	527 ± 8	9.8	0.69816 ± 0.01265	0.08524 ± 0.00068	0.44
57	2	74	175	529 ± 10	522 ± 6	6.6	0.68351 ± 0.00894	0.08440 ± 0.00056	0.51
58	14R	17	76	545 ± 20	523 ± 10	18.2	0.70972 ± 0.01713	0.08458 ± 0.00082	0.40
59	17	27	87	515 ± 36	523 ± 12	28.9	0.66062 ± 0.02930	0.08443 ± 0.00103	0.28
60	22	40	150	53 6 ± 12	527 ± 8	8.7	0.69566 ± 0.01036	0.08521 ± 0.00062	0.49
61	23	54	161	545 ± 16	522 ± 8	19.7	0.71107 ± 0.01415	0.08437 ± 0.00075	0.45
62	24	62	194	537 ± 12	521 ± 8	14.9	0.69725 ± 0.01004	0.08414 ± 0.00061	0.50
63	25R	48	158	556 ± 12	525 ± 8	24.2	0.72861 ± 0.01044	0.08485 ± 0.00061	0.50
64	30C	23	75	551 ± 24	525 ± 12	21.7	0.72131 ± 0.02018	0.08481 ± 0.00094	0.40
65	34	46	152	536 ± 12	525 ± 8	10.4	0.69477 ± 0.00983	0.08478 ± 0.00059	0.49
66	48	34	100	533 ± 16	521 ± 8	10.6	0.68956 ± 0.01352	0.08425 ± 0.00071	0.43
67	42	28	97	536 ± 18	528 ± 8	7.0	0.69460 ± 0.01423	0.08541 ± 0.00074	0.42
68	10R	89	214	581 ± 22	523 ± 8	48.5	0.77200 ± 0.01975	0.08450 ± 0.00072	0.33
69	12	69	185	552 ± 20	515 ± 8	44.9	0.72152 ± 0.01722	0.08310 ± 0.00069	0.35
70	18C	11	46	604 ± 38	525 ± 16	44.0	0.81223 ± 0.03325	0.08493 ± 0.00137	0.39
71	20	74	231	639 ± 40	528 ± 18	51.8	0.87647 ± 0.03681	0.08543 ± 0.00145	0.40
72	25C	30	91	513 ± 22	512 ± 10	1.2	0.65721 ± 0.01736	0.08264 ± 0.00085	0.39
73	32	727	902	515 ± 10	501 ± 6	13.3	0.66032 ± 0.00819	0.08080 ± 0.00054	0.54
74	39	45	93	487 ± 28	453 ± 12	31.3	0.61594 ± 0.02151	0.07286 ± 0.00098	0.39
75	35C*	31	87	558 ± 20	535 ± 10	18.9	0.73262 ± 0.01722	0.08653 ± 0.00083	0.41
76	26C*	27	78	564 ± 20	535 ± 10	22.8	0.74339 ± 0.01707	0.08653 ± 0.00082	0.41
77	44*	168	248	559 ± 18	538 ± 8	17.5	0.73443 ± 0.01452	0.08704 ± 0.00074	0.43
78	51*	50	161	549 ± 12	539 ± 8	9.0	0.71724 ± 0.01048	0.08724 ± 0.00062	0.49
79	52*	43	161	546 ± 14	536 ± 8	9.9	0.71275 ± 0.0115	0.08663 ± 0.00066	0.47
Plagiogranite association, late phase, plagiogranite, sample PM-28-14									
80	2R	55	184	522 ± 18	520 ± 10	1.6	0.67156 ± 0.01499	0.08404 ± 0.00077	0.41
81	3R	69	249	537 ± 16	523 ± 8	12.4	0.69657 ± 0.01296	0.08457 ± 0.00072	0.46
82	5	45	150	522 ± 10	524 ± 6	–2.3	0.67230 ± 0.00748	0.08471 ± 0.00055	0.58

(*continued on next page*)

Table 4 (*continued*)

No.	Point	Th	U	Age, Ma, ± 2δ		Discordance, %	$^{207}Pb/^{235}U$, ± 1δ	$^{206}Pb/^{238}U$, ± 1δ	Rho
		ppm		$^{207}Pb/^{235}U$	$^{206}Pb/^{238}U$				
Plagiogranite association, late phase, plagiogranite, sample PM-28-14									
83	8C	57	162	528 ± 32	521 ± 10	6.8	0.68146 ± 0.02661	0.08414 ± 0.00091	0.28
84	11R	40	172	541 ± 12	519 ± 8	19.2	0.70441 ± 0.00937	0.08386 ± 0.00062	0.56
85	11C	38	147	521 ± 10	525 ± 6	–4.7	0.67079 ± 0.00852	0.08492 ± 0.00058	0.54
86	12R	44	204	532 ± 14	526 ± 8	6.2	0.68877 ± 0.01093	0.08499 ± 0.00064	0.47
87	13C	122	320	520 ± 10	520 ± 6	0	0.66845 ± 0.00806	0.08397 ± 0.00055	0.54
88	13R	28	144	523 ± 20	521 ± 10	2.5	0.67353 ± 0.01611	0.08410 ± 0.00081	0.40
89	17	47	153	529 ± 14	519 ± 8	9.5	0.68337 ± 0.01089	0.08385 ± 0.00064	0.48
90	20	67	177	550 ± 10	525 ± 6	20.7	0.71899 ± 0.00918	0.08487 ± 0.00057	0.53
91	21	34	137	563 ± 10	523 ± 6	29.3	0.74088 ± 0.00864	0.08450 ± 0.00057	0.58
92	23C	47	195	516 ± 22	521 ± 8	–6.1	0.66247 ± 0.01788	0.08425 ± 0.00074	0.33
93	25	19	95	541 ± 18	528 ± 8	11.6	0.70309 ± 0.01479	0.08535 ± 0.00066	0.37
94	27	39	149	539 ± 10	526 ± 6	12.1	0.70041 ± 0.00812	0.08500 ± 0.00055	0.56
95	34	29	97	536 ± 14	523 ± 8	12.6	0.69570 ± 0.01176	0.08445 ± 0.00065	0.46
96	4C	12	72	525 ± 18	515 ± 8	10.5	0.67755 ± 0.01437	0.08309 ± 0.00067	0.38
97	9C	22	94	549 ± 18	526 ± 8	19.0	0.71684 ± 0.01577	0.08505 ± 0.00066	0.35
98	9R	38	180	507 ± 12	527 ± 8	–27.5	0.64745 ± 0.01011	0.08520 ± 0.00064	0.48
99	33C	18	92	518 ± 36	528 ± 14	–11.2	0.66602 ± 0.03016	0.08532 ± 0.00110	0.28
100	2C*	73	255	542 ± 14	535 ± 8	6.6	0.70481 ± 0.01168	0.08650 ± 0.00066	0.46
101	4R*	12	70	559 ± 28	538 ± 14	16.8	0.73334 ± 0.02433	0.08711 ± 0.00111	0.38
102	12C*	35	158	538 ± 12	535 ± 8	3.5	0.69941 ± 0.00987	0.08653 ± 0.00060	0.49
103	15*	45	143	551 ± 12	543 ± 8	7.4	0.72070 ± 0.01038	0.08789 ± 0.00062	0.49
104	30C*	17	87	615 ± 24	537 ± 10	42.7	0.83185 ± 0.02129	0.08692 ± 0.00092	0.41
Dut Uul pluton Plagiogranite association, plagiogranite, sample PM-62-08									
105	7	110	357	469 ± 14	472 ± 8	–5	0.58662 ± 0.01091	0.07604 ± 0.00062	0.44
106	9	178	268	498 ± 16	494 ± 8	4	0.63278 ± 0.01359	0.07970 ± 0.00073	0.43
107	15	107	275	515 ± 14	508 ± 8	7.5	0.66100 ± 0.01222	0.08201 ± 0.00068	0.45
108	2*	45	136	549 ± 14	540 ± 8	8.2	0.71752 ± 0.01222	0.08745 ± 0.00068	0.46
109	8*	60	160	526 ± 16	531 ± 8	–5.8	0.67898 ± 0.01360	0.08594 ± 0.00075	0.44
110	10*	114	301	540 ± 14	538 ± 8	2.0	0.70125 ± 0.01212	0.08697 ± 0.00070	0.47
111	3*	437	1807	374 ± 44	255 ± 6	89.7	0.44495 ± 0.03075	0.04041 ± 0.00048	
112	4*	95	694	254 ± 40	250 ± 6	88.7	0.28377 ± 0.02571	0.03948 ± 0.00047	0.17
113	5*	105	316	503 ± 28	507 ± 10	36.9	0.64143 ± 0.02298	0.08177 ± 0.00077	0.13
114	6*	523	900	723 ± 26	456 ± 8	76.5	1.03799 ± 0.02690	0.07337 ± 0.00062	0.26
115	11*	2291	2200	529 ± 34	226 ± 4	93	0.68303 ± 0.02846	0.03570 ± 0.00037	0.25
116	13*	264	543	480 ± 36	399 ± 8	72.9	0.60483 ± 0.02816	0.06380 ± 0.00071	0.21
117	14*	295	343	517 ± 20	487 ± 10	26.4	0.66368 ± 0.01558	0.07843 ± 0.00077	0.42
118	16*	129	382	416 ± 38	410 ± 10	60.5	0.50601 ± 0.02871	0.06572 ± 0.00081	0.22
119	17*	10410	3154	777 ± 14	237 ± 4	93.7	1.14849 ± 0.01852	0.03751 ± 0.00031	0.51
120	19*	204	522	491 ± 14	466 ± 10	24.5	0.62171 ± 0.01675	0.07493 ± 0.00082	0.41

Note. The U–Pb dating of single zircon grains was performed by ICP MS on an Agilent 7700cx quadruple mass spectrometer equipped with a Photon Machines Excite Excimer laser ablation system (λ = 193 nm) at the Analytical Center of GEMOC (Department of Earth and Planetary Science, Macquarie University, Sydney, Australia), following the technique described by Griffin et al. (2004), Jackson et al. (2004), and Belousova et al. (2009). Cathodoluminescence images showing the internal structure and zoning of zircons were used to choose grain surface sites for dating. Operating conditions: helium atmosphere, laser beam diameter 40–65 μm, frequency 5 Hz, and laser energy density 2.8–5.6 mJ/pulse. Each measurement lasted 3 min and comprised the background (2 min) and signal (1 min) measurement. The measurements were made in runs of 14 analyses, which comprised ten analyses of the zircons under study and two analyses of the GEMOC GJ-1 zircon standard (Elhlou et al., 2006) at the beginning and at the end of each run. Two other well-studied zircon standards, 91500 (Wiedenbeck et al., 1995) and Mud Tank (Black and Gulson, 1998), were also analyzed in each run to control the reproducibility of the results and the stability of the instrument operation. Correction for common lead was made following to Andersen et al. (2002). The U–Pb age was calculated using the GLITTER software (www.mq.edu.au/GEMOC; Griffin et al., 2004), which permits recognition of isotopically homogeneous signal segments.

* The number of points at which isotope measurements for xenogenic zircons were made; the rest points correspond to isotope measurements for magmatic zircons.

zircons. The grains of inherited zircon are overgrown with wide rims of newly formed magmatic zircon with an age of 515–526 Ma corresponding to the magmatic stage of crystallization of plagiogranitic melt (see above). This indicates that the zircon stayed for a long time in the crystallizing plagiogranitic melt (probably, at the depth of generation of the parental melts). The thin white rims at the boundary between the inherited and newly formed zircons apparently indicate recrystallization of the former zircons as a result of their interaction with hot granitic melts. Analyses were carried out for four grains of the inherited zircon (Table 4, Nos. 100–103). Their Th/U ratios are 0.20–0.31. The U–Pb isotope studies of these grains show their $^{206}Pb/^{238}U$ age of 543–535 Ma, and the weighted average age is 538 ± 5 Ma (MSWD = 0.89). Taking into account the resorbed nature of the edges and faces of the inherited zircons and their ages, as well as their overgrowth with wide rims of newly formed magmatic zircon, we can consider the rocks with zircons of this age (538 ± 5 Ma) an additional source of matter during the generation of the parental melts for plagiogranitoids of the early and late phases of the Bayasgalant pluton.

The Dut Uul pluton. To determine the age of the pluton rocks, we studied a monofraction of zircon from medium-grained gneissoid biotite–amphibole plagiogranites (Fig. 3, sample PM-62-08). This zircon has pink to colorless transparent euhedral crystals of a prismatic habit (50–300 μm in size; K_l = 2.0–3.5). The CL images (Fig. 5) show a thin magmatic zoning in the crystals. Analyses of 13 grains of magmatic zircon show Th/U = 0.26–0.76 (Table 3 and Table 4, Nos. 105–107). The concordant $^{206}Pb/^{238}U$ age (Table 3; Fig. 6) calculated over 10 points is 481 ± 5 Ma (MSWD = 0.02).

A specific feature of this monofraction is the presence of relics of "ancient" zircon cores, mostly as elongate grains (50–150 μm in size, K_l = 2–4, Fig. 5) with clear signs of resorption of the edges and faces and their overgrowth with the later generation of zircon marking the crystallization of granitic melt (see above). These specific features of the "ancient" zircon cores testify to their inherited nature. As seen from Fig. 5, the zircons have a rough magmatic zoning, and some grains are structureless and dark. Analyses of 20 grains of inherited zircons (Table 4, Nos. 108–120) showed a wide variation in the contents of Th and U (Th/U = 0.14–3.3). Only three grains of xenogenic zircon (Table 4, Nos. 108–110), which have preserved the internal structure, show more stable contents of Th and U (Th/U = 0.38) and age values (540–526 Ma). The concordant age for these inherited zircons is 537 ± 2 Ma (MSWD = 0.36), and the weighted average age is 536 ± 9 Ma (MSWD = 0.35).

DISCUSSION

Analysis of the stages of formation of plagiogranitoids and their geodynamic setting. The results of geochronological studies show that plagiogranitoid associations composing different intrusive areas in the south of the Lake Zone (the axial part of its island-arc system) formed over the long period 531–481 Ma. This indicates different times of formation of the rock associations united into the early Cambrian Tohtogenshil complex. The early Paleozoic intrusive associations in the south of the Lake Zone are close in the duration of formation to the plagiogranitod associations of the island-arc and accretion–collision stages of evolution of the northern and central parts of the Lake Zone (Bumbat Hayrhan area—551–468 Ma, Har Nuur—530–460 Ma, and Hyargas Nuur—519–494 Ma, Table 1) (Kovalenko et al., 2004; Rudnev et al., 2009, 2012; Yarmolyuk et al., 2011).

Thus, taking into account the above data on the geologic structure of the plagiogranitoid associations, their relationship with the host rocks, and their age as well as the regional specifics of intrusive (granitoid and gabbroid) magmatism in other areas of the Lake Zone, we conclude that these associations formed at two geodynamic stages of the regional evolution: island-arc (531–517 Ma) and accretion–collision (504–481 Ma).

The island-arc stage (531–517 Ma). Diorite–tonalite–plagiogranite associations were the most widespread in this period, and plagiogranite associations were subordinate. According to the results of geochronological studies, the island-arc associations formed at two stages of the evolution of the Lake Zone island arc. The early-phase rocks of the Tugrug pluton (531 ± 4 Ma, Figs. 3 and 6) formed at the early stage of plagiogranitic magmatism, and the rocks of the Udzur-Hunga (517 ± 4 Ma), Hatan-Hunga (521 ± 3 Ma), and Bayasgalant (early phase—524 ± 4 Ma, late phase—522 ± 2 Ma) plutons, at the late stage.

Gabbroid associations are closely conjugate with plagiogranitoids in space and time and are always older. This is indicated by the geologic relationships (Fig. 3) of gabbroids of the Tuguruk pluton (Izokh et al., 1990) and later formed rocks of the diorite–tonalite–plagiogranite association of the early phase of the Tugrug pluton (531 ± 4 Ma) (Rudnev et al., 2013a)) with plagiogranites of the Hatan-Hunga pluton (521 ± 3 Ma) and by the presence of gabbroid xenoliths in plagiogranitoids. The geochronological age of gabbroids of the Hyargas Nuur complex in the magmatic areas in the south of the Lake Zone is still unclear, but we can state that gabbroids of the Tuguruk pluton are no younger than 531 Ma. At the same time, all the above plagiogranitoid plutons have postgranitic diabase dikes of two ages (e.g., the Tugrug pluton), which suggests the existence of zones of basic (gabbroid) magmatism of other ages.

Mineralogical and petrographic studies have shown two petrographic types of plagiogranitoid associations formed at the island-arc stage: biotite–amphibole and muscovite–biotite. Biotite–amphibole plagiogranitoids usually form long completed intrusive series (quartz diorites, tonalites, plagiogranites, and leucoplagiogranites) with a significant predominance of quartz diorites or tonalites, as, e.g., in the Tugrug, Udzur-Hunga, and Bayasgalant plutons. Muscovite–biotite plagiogranitoids, e.g., plagiogranites and leucoplagiogranites of the Hatan-Hunga pluton (Fig. 3), lack more basic varieties (tonalites and quartz diorites).

In general, in age and mineral and petrographic compositions the island-arc plagiogranitoid associations in the south of the Lake Zone are almost identical to the island-arc plagiogranitoid associations in the intrusive areas of the northern and central parts of this zone. For example, the rocks of the diorite–tonalite–plagiogranite association of the Udzur-Hunga (517 ± 2 Ma) and Bayasgalant plutons (524 ± 4 Ma, early phase) are almost analogous in age and mineral and petrographic compositions to the plagiogranitoids of the Sharathologoy pluton (519 ± 8 Ma; Table 1, Fig. 2) in the Hyargas Nuur area in the north of the Lake Zone and to plagiogranitoids of the Dariv pluton (524 ± 10 Ma) in the Bumbat Hayrhan area in the central part of the Lake Zone (Rudnev et al., 2009, 2012). Muscovite–biotite plagiogranites and leucoplagiogranites of the Hatan–Hunga pluton (521 ± 6 Ma) are similar in age (within the analytical error) and mineral and petrographic compositions to plagiogranites and leucoplagiogranites of the Har Nuur pluton (531 ± 10 Ma) and to muscovite–biotite plagiogranites of the Bumbat Hayrhan pluton (535 ± 6 Ma) in the northern and central parts of the Lake Zone.

There are also other intrusive associations in the early Caledonian structures of the Lake Zone which are similar in age to the above plagiogranitoid and gabbroid associations. Among them are a number of small plutons in the area of the Haan Tayshiri Range. According to geochronological studies (Janoušek et al., 2018), the age of gabbroids, quartz diorites, and tonalites of these plutons is 538–516 Ma (Table 1).

The accretion–collision stage (504–481 Ma) of granitoid magmatism in the south of the Lake Zone was not as global as the island-arc stage (Figs. 2 and 3). Geological and geochronological data show a predominance of plagiogranite–leucoplagiogranite associations and, to a lesser extent, tonalite–plagiogranite and diorite–tonalite–plagiogranite associations at this geodynamic stage of evolution of the above area. The earliest are muscovite–biotite plagiogranites and leucoplagiogranites of the Tugrug pluton (Tugrug area, late phase, 504 ± 4 Ma), which are similar in mineral and petrographic compositions to biotite (±muscovite) plagiogranites and leucoplagiogranites of the Dut Uul pluton (481 ± 3 Ma). At the same time, the rocks of these plutons do not differ in textures, structures, and mineral and petrographic compositions from the muscovite–biotite plagiogranites and leucoplagiogranites of the Hatan-Hunga pluton (521 ± 6 Ma), formed at the island-arc stage. The rocks of diorite–tonalite–plagiogranite association of the Mandalt pluton are similar in the set of rock groups and mineral and petrographic compositions to plagiogranitoids of the Udzur-Hunga and Tugrug plutons (early phase) but differ in the age (495 ± 8 Ma) and geodynamic setting. All this once again demonstrates that granitoids with the same mineral and petrographic compositions might be of different ages and might have formed in different geodynamic settings.

The above plagiogranitoid associations of the accretion–collision stage (504–481 Ma) have age analogs among granitoids (498–467 Ma) (Kozakov et al., 2002; Jahn et al., 2014) in the area of the junction (obduction) of late Neoproterozoic–early Cambrian volcanic complexes of the back-arc part of the Lake Zone island-arc system with Precambrian rocks of the Dzavhan microcontinent in the area of the Dariv Range (Fig. 2) and among diorites, quartz diorites, and granodiorites (511–495 Ma, Table 1) of the Haan Tayshiri Range (Janoušek et al., 2018).

U–Pb isotope studies of xenogenic and inherited zircons. Studies of xenogenic and inherited zircons (Rudnev et al., 2018) showed their isotopic age of 664 to 520 Ma (Tables 3 and 4; Fig. 6). The zircons can be conventionally divided into four groups by age. Surely, the available quantity of xenogenic and inherited zircons is not enough for a generalized analysis. Therefore, the performed geochronological studies provide only the first ideas of the time interval of formation of the rocks that can be considered additional sources of matter during the granite formation.

The first and second groups include inherited zircons, i.e., those borrowed by melt from the sources that were directly involved in melting during the generation of parental plagiogranitic melts. These zircons are of limited occurrence and are found only as single grains.

The first group is inherited zircons with an age of 664 ± 18 Ma. They were found in island-arc plagiogranites of the Hatan-Hunga pluton, dated at 521 ± 3 Ma (Figs. 5 and 6). Judging from the magmatic nature and morphology (rounded grains) of this zircon, it is, most likely, a product of destruction and ablation of intrusive rocks (volcanics and their tuffs, gabbroids, and plagiogranitoids) of ophiolite complexes. This is also indicated by the close ages of inherited zircons from anorthosites (665 ± 15 and 655 ± 4 Ma), plagiogranites, and the host volcanics in the Bayan Hongor ophiolite belt (Kovach et al., 2005; Jian et al., 2010). Probably, the sedimentary rocks that resulted from the destruction of rocks of ophiolite complexes (e.g., Bayan Hongor), together with MORB-type metabasites, were involved in the melting during the subduction of the oceanic plate. As a result, parental melts for plagiogranites of the Hatan–Hunga pluton formed.

The second group is inherited zircons with an age of 563 ± 6 Ma (Fig. 6), which are fragments of well-rounded crystals with preserved magmatic zoning (Fig. 5). Such zircons are present only in late-phase plagiogranites of the Tugrug pluton (504 ± 3 Ma), formed at the accretion–collision stage of evolution of the Lake Zone. Taking into account the magmatic origin of xenogenic zircon and its isotopic age, we assume that it was supplied from sedimentary rocks that resulted from the destruction and ablation of intrusive and volcanic complexes of late Neoproterozoic age (570–560 Ma). Based on the geologic structure of the Lake Zone and adjacent geoblocks (terranes), we think that the sedimentary rocks that resulted from the destruction and ablation of igneous rocks (gabbroids, plagiogranites, volcanics and their tuffs) of these geoblocks might have been addi-

tional magma-generating sources for late-phase plagiogranites of the Tugrug pluton. This is indirectly confirmed by rocks of the Bayan Nuur ophiolite complex of the Dariv Range (565–560 Ma, Figs. 1 and 2, Table 1), Haan Tayshiri ophiolite complex (573–565 Ma), and Bayan Hongor ophiolite complex (577–569 Ma) and by the host island-arc and oceanic volcanic deposits of late Neoproterozoic age (~570 Ma) (Kepezhinskas et al., 1991; Gibsher et al., 2001; Kozakov et al., 2002; Terent'eva et al., 2010; Yarmolyuk et al., 2011; Jian et al., 2014).

The third group is inherited zircons with an age of 545–531 Ma (Table 4). They are the most common and have mainly prismatic and subeuhedral crystals with magmatic zoning. Inherited zircons of this group are found in plagiogranitoids of the Hatan-Hunga pluton (521 ± 3 Ma) and the Bayasgalant pluton (early and late phases, 524–522 Ma), formed at the final stage of the island-arc evolution in the Lake Zone, and in plagiogranites of the Dut Uul pluton (481 ± 3 Ma), formed at the accretion–collision stage of the regional evolution. The isotopic ages estimated from these inherited zircons with regard to their magmatic genesis are close to the age of the plagiogranitoid and gabbroid associations (complexes) formed at the early stage of evolution of the Lake Zone island arc (535–529 Ma (Rudnev et al., 2009, 2012, 2016)) and to the late Neoproterozoic–early Cambrian age (546 ± 3 Ma) of volcanic and volcanosedimentary island-arc deposits (Yarmolyuk et al., 2011). There are also intrusive rocks of similar age (Table 1; Fig. 2): plagiogranitoids of the Tugrug pluton (531 ± 4 Ma), preceding gabbroids of the Tuguruk pluton and plagiogranitoids of the Bumbat Hayrhan (535 ± 6 Ma) and Har Nuur (529–531 Ma) plutons in the central and northern parts of the Lake Zone, and gabbroids and diorites of the Haan Tayshiri and Zamtyn Nuruu Ranges in the south of the Lake Zone (542–538 Ma, Table 1) (Buriánek et al., 2017; Janoušek et al., 2018). The similar ages of the inherited zircon and the granitoids and volcanics formed at the early stages of evolution of the Lake Zone island arc suggest that the parental melts for plagiogranitoids of the Hatan-Hunga, Basgalant, and Dut Uul plutons were generated under the certain influence of sedimentary rocks resulted from the destruction and ablation of island-arc rocks.

The fourth group unites zircons with an age of 519–530 Ma. They are found in plagiogranitoids formed at the accretion–collision stage of evolution of the Lake Zone (Tugrug and Mandalt plutons). These zircons are xenogenic and inherited. Xenogenic zircons are present in plagiogranitoids of the Mandalt pluton (495 ± 8 Ma). Their age varies from 530 to 519 Ma (the weighted average age is 522 ± 6 Ma, Fig. 6). Inherited zircons with an age of ~524 Ma occur in late-phase plagiogranites of the Tugrug pluton (504 ± 3 Ma). Zircons of both types are prismatic subeuhedral, with magmatic zoning. In contrast to the xenogenic zircons, the inherited zircons have wide rims of newly formed zircon indicating their long-term existence in the crystallizing granitic melt. The ages of the inherited and xenogenic zircons from rocks of the above plutons are similar to the ages of island-arc plagiogranitoids of the Udzur-Hunga, Hatan-Hunga, and Bayasgalant plutons (517 ± 4, 521 ± 3, and 524–523 Ma, respectively), plagiogranitoids of the Bumbat Hayrhan and Sharatologoy plutons (524 ± 10 and 519 ± 8 Ma, respectively) in the northern and central parts of the same island-arc belt, and gabbroids, quartz diorites, and tonalites of the Haan Tayshiri Range (524–516 Ma, Table 1, Fig. 1) (Rudnev et al., 2009, 2012, 2016; Buriánek et al., 2017; Janoušek et al., 2018). Taking into account the similar ages, we suggest that these inherited zircons were borrowed by the melt from sedimentary deposits resulted from the destruction and ablation of island-arc rocks. During the tectonic processes at the collision stage of the Lake Zone evolution, these sedimentary deposits, along with blocks of tectonically mixed island-arc and oceanic rocks, got into the lower parts of collisional structures, where they were involved in melting under the effect of the heat of ascending mantle melts. As a result, parental melts for plagiogranites of the Tugrug and Mandalt plutons were generated. In contrast to the inherited zircons from the Tugrug pluton, the xenogenic zircons from plagiogranites of the Mandalt pluton occur as individual grains but lack obvious signs of melting and overgrowth with newly formed zircon. This apparently indicates that they were borrowed from the host rocks at the pluton formation depth.

Thus, the results of study of xenogenic and inherited zircons from plagiogranitoids of the southern part of the Lake Zone have led us to the following important conclusions:

(1) Xenogenic and inherited zircons are older than 664–52 Ma. This means that during the formation of plagiogranitoids at the island-arc and accretion–collision stages of the regional evolution (531–481 Ma), the composition of parental melts was influenced by sedimentary rocks resulted from the destruction and ablation of intrusive and volcanic island-arc and ophiolite complexes with ages of 565–535 and 664 Ma.

(2) The absence of xenogenic and inherited zircons older than 664 Ma also indicates that Precambrian structures (e.g., the Dzavhan microcontinent) did not influence the composition of melts that generated plagiogranitoids at the island-arc and accretion–collision stages of evolution of the southern part of the Lake Zone. This means that the island-arc complexes of the Lake Zone formed far from the ablation areas of Precambrian blocks (microcontinents), which is also evidenced from the results of paleomagnetic studies (Kurenkov et al., 2002; Kheraskova et al., 2010). At the later accretion–collision stage, when the accretion of island arcs, back-arc basins, and microcontinents (Dzavhan) began, parental plagiogranitic melts formed, most likely, without a significant contribution of Precambrian sedimentary material. The source of parental melts might have contained only pelitic material supplied from the Dzavhan microcontinent.

To confirm these conclusions, we must perform additional analytical studies, including geochemical ones, and Sr–Nd and Hf isotope research. We will report their results in the next paper.

CONCLUSIONS

(1) The results of geochronological studies indicate that plagiogranitoid associations in the south of the Lake Zone formed in the period from 531 to 481 Ma. There were two stages of intrusive magmatism in this period, which correspond to two major stages of the zone evolution: island-arc, 531–517 Ma, and accretion–collision, 504–481 Ma. In the south of the Lake Zone, in contrast to its northern and central parts, plagiogranitoid associations of the island-arc stage are most widespread. Magmatism of the accretion–collision stage was manifested on a much smaller scale here.

(2) At all stages, granitoid associations of the tonalite–trondhjemite series were predominant. By petrochemical composition they are assigned to calc-alkalic rocks.

(3) The study of xenogenic and inherited zircons from early Paleozoic plagiogranitoids formed at the island-arc and accretion–collision stages of evolution of the southern part of the Lake Zone has shown their age range 664–520 Ma. Four age groups of xenogenic and inherited zircons have been recognized (~664, 570–560, 545–531, and 530–520 Ma), which generally correspond to the stages of island-arc (volcanic and intrusive) and ophiolite magmatism and apparently reflect the additional magma-generating sources of parental plagiogranitic melts.

(4) The absence of xenogenic and inherited zircons older than 664 Ma from early Paleozoic plagiogranitoids in the south of the Lake Zone (axial part) also indicates that Precambrian structures did not affect the compositions of parental plagiogranitic melts and the remoteness of the island arc of the Lake Zone from the ablation areas of Precambrian blocks.

We are deeply grateful to R.A. Shelepaev for help in the field research, E.A. Kruk (V.S. Sobolev Institute of Geology and Mineralogy, Novosibirsk) for processing of stone materials and map documents, N.G. Karmanova and A.N. Toryanik (V.S. Sobolev Institute of Geology and Mineralogy, Novosibirsk), E.N. Lepekhina, A.N. Larionov, N.V. Rodionov, N.G. Berezhnaya, and A.V. Antonov (A.P. Karpinsky Russian Geological Research Institute, St. Petersburg) for participation in analytical studies, and O.M. Turkina and T.V. Donskaya for valuable remarks.

The work is done on state assignment of the V.S. Sobolev Institute of Geology and Mineralogy, SB RAS, and with a financial support by grants 18-05-00105 and 15-05-05615 from the Russian Foundation for Basic Research.

REFERENCES

Andersen, T., 2002. Correction of common Pb in U–Pb analyses that do not report ^{204}Pb. Chem. Geol. 192, 59–79.

Badarch, G., Cunningham, W.D., Windley, B.F., 2002. A new terrane subdivision for Mongolia: Implications for the Phanerozoic crustal growth of Central Asia. J. Asian Earth Sci. 21, 87–104.

Belousova, E.A., Reid, A.J., Griffin, W.L., O'Reilly, S.Y., 2009. Rejuvenation vs. recycling of Archean crust in the Gawler Craton, South Australia: evidence from U–Pb and Hf isotopes in detrital zircon. Lithos 113, 570–582.

Black, L.P., Gulson, B.L., 1978. The age of the Mud Tank Carbonatite, Strangways Range, Northern Territory. Bur. Mineral. Resour. J. Aust. Geol. Geophys. 3, 227–232.

Black, L.P., Kamo, S.L., Allen, C.M., Aleinikoff, J.N., Davis, D.W., Korsch, R.J., Foudoulis, C., 2003. TEMORA 1: A new zircon standard for U–Pb geochronology. Chem. Geol. 200, 155–170.

Buriánek, D., Schulmann, K., Hrdličková, K., Hanžl, P., Janoušek, V., Gerdes, A., Lexa, O., 2017. Geochemical and geochronological constraints on distinct Early-Neoproterozoic and Cambrian accretionary events along southern margin of the Baydrag Continent in western Mongolia. Gondwana Res. 47, 200–227.

Dergunov, A.B., 1989. The Caledonides of Central Asia [in Russian]. Nauka, Moscow, pp. 1–192.

Dergunov, A.B., Kovalenko, V.I., Ruzhentsev, S.V., Yarmolyuk, V.V., 2001. Tectonics, Magmatism, and Metallogeny of Mongolia. Routledge, London, New York.

Dijkstra, A.H., Brouwer, F.M., Cunningham, W.D., Buchan, C., Badarch, G., Mason, P.R.D., 2006. Late Neoproterozoic proto-arc ocean crust in the Dariv Range, Western Mongolia: a supra-subduction zone end-member ophiolite. J. Geol. Soc. 163, 363–373.

Elhlou, S., Belousova, E., Griffin, W.L., Pearson, N.J., O'Reilly, S.Y., 2006. Trace element and isotopic composition of GJ-red zircon standard by laser ablation. Geochim. Cosmochim. Acta 70, A158.

Frost, B.R., Barnes, C.G., Collins, W.J., Arculus, R.J., Ellis, D.J., Frost, C.D., 2001. A geochemical classification for granitic rocks. J. Petrol. 42, 2033–2048.

Gibsher, A.S., Khain, E.V., Kotov, A.B., Sal'nikova, E.B., Kozakov, I.K., Kovach, V.P., Yakovleva, S.Z., Fedoseenko, A.M., 2001. Late Vendian age of the Han-Taishiri ophiolite complex in western Mongolia. Geologiya i Geofizika (Russian Geology and Geophysics) 42 (8), 1179–1185 (1110–1117).

Gordienko, I.V., 2006. Geodynamic evolution of late Baikalides and Paleozoids in the folded periphery of the Siberian craton. Russian Geology and Geophysics (Geologiya i Geofizika) 47 (1), 51–67 (53–70).

Griffin, W.L., Belousova, E.A., Shee, S.R., Pearson, N.J., O'Reilly, S.Y., 2004. Archean crustal evolution in the northern Yilgarn Craton: U–Pb and Hf-isotope evidence from detrital zircons. Precambrian Res. 131, 231–282.

Izokh, A.E., Polyakov, G.V., Krivenko, A.P., Bognibov, V.I., Bayarbileg, L., 1990. Gabbroid Associations of Western Mongolia [in Russian]. Nauka, Novosibirsk.

Izokh, A.E., Polyakov, G.V., Gibsher, A.S., Balykin, P.A., Zhuravlev, D.Z., Parkhomenko, V.A., 1998. High-alumina stratified gabbroids of the Central-Asian fold belt: geochemistry, Sm–Nd isotopic age, and geodynamic conditions of formation. Geologiya i Geofizika (Russian Geology and Geophysics) 39 (11), 1565–1577 (1565–1577).

Jackson, S.E., Pearson, N.J., Griffin, W.L., Belousova, E.A., 2004. The application of laser ablation–inductively coupled plasma-mass spectrometry to in situ U–Pb zircon geochronology. Chem. Geol. 211, 47–69.

Jahn, B.M., 2004. The Central Asian Orogenic Belt and growth of the continental crust in the Phanerozoic, in: Malpas, J., Fletcher, C.J.N., Aitchison, J.C. (Eds.), Aspects of the Tectonic Evolution of China. Geol. Soc. London, Spec. Publ. 226, 73–100.

Jahn, B.M., Wu, F., Chen, B., 2000a. Granitoids of the Central Asian Orogenic Belt and continental growth in the Phanerozoic. Trans. R. Soc. Edinburgh 91, 181–193.

Jahn, B.M., Wu, F., Chen, B., 2000b. Massive granitoid generation in Central Asia: Nd isotope evidence and implication for continental growth in the Phanerozoic. Episodes 23, 82–92.

Janoušek, V., Jiang, Y., Buriánek, D., Schulmann, K., Hanžl, P., Soejono, I., Kröner, A., Altanbaatar, B., Erban, V., Lexa, O., Ganchu-

luun, T., Košler, J., 2018. Cambrian–Ordovician magmatism of the Ikh-Mongol Arc System exemplified by the Khantaishir Magmatic Complex (Lake Zone, south–central Mongolia). Gondwana Res. 54, 122–149.

Jian, P., Kröner, A., Windley, B.F., Shi, Y., Zhang, F., Miao, L., Tojurhuu, D., Zhang, W., Liu, D., 2010. Zircon ages of the Bayankhongor ophiolite mélange and associated rocks: time constraints on Neoproterozoic to Cambrian accretionary and collisional orogenesis in Central Mongolia. Precambrian Res. 177, 162–180.

Jian, P., Kröner, A., Jahn, B.-M., Windley, B.F., Shi, Y., Zhang, W., Zhang, F., Miao, L., Tomurhuu, D., Liu, D., 2014. Zircon dating of Neoproterozoic and Cambrian ophiolites in West Mongolia and implications for the timing of orogenic processes in the central part of the Central Asian Orogenic Belt. Earth Sci. Rev. 133, 62–93.

Kepezhinskas, P.K., Kepezhinskas, K.B., Puchtel, I.S., 1991. Lower Paleozoic oceanic crust in Mongolian Caledonides: Sm–Nd isotope and trace element data. Geophys. Res. Lett. 18 (7), 1301–1304.

Khain, E.V., Amelin, Yu.V., Izokh, A.E., 1995. Sm-Nd data on the age of ultramafic-mafic complexes in subduction zone of Western Mongolia. Dokl. Akad. Nauk 341 (6), 791–796.

Kheraskova, T.N., Bush, V.A., Didenko, A.N., Samygin, S.G., 2010. Breakup of Rodinia and early stages of evolution of the Paleoasian Ocean. Geotectonics 44 (1), 3–24.

Kovach, V.P., Yarmolyuk, V.V., Kozakov, I.K., Terent'eva, L.B., Lebedev, V.I., Kovalenko, V.I., 2005. Magmatism and geodynamics of early stages of the Paleoasian Ocean formation: geochronological and geochemical data on ophiolites of the Bayan-Khongor zone. Dokl. Earth Sci. 404 (7), 1072–1077.

Kovach, V.P., Yarmolyuk, V.V., Kovalenko, V.I., Kozlovskyi, A.M., Kotov, A.B., Terent'eva, L.B., 2011. Composition, sources, and mechanisms of formation of the continental crust of the Lake Zone of the Central Asian Caledonides. II. Geochemical and Nd isotope data. Petrology 19 (4), 399–425.

Kovalenko, V.I., Yarmolyuk, V.V., Kovach, V.P., Kotov, A.B., Kozakov, I.K., Sal'nikova, E.B., 1996. Sources of Phanerozoic granitoids of Central Asia: Sm–Nd isotope data. Geokhimiya, No. 8, 699–712.

Kovalenko, V.I., Yarmolyuk, V.V., Sal'nikova, E.B., Kartashov, P.M., Kovach, V.P., Kozakov, I.K., Kozlovskii, A.M., Kotov, A.B., Ponomarchuk, V.A., Listratova, E.N., Yakovleva, S.Z., 2004. The Khaldzan–Buregtei massif of peralkaline rare-metal igneous rocks: structure, geochronology, and geodynamic setting in the Caledonides of Western Mongolia. Petrology 12 (5), 412–436.

Kovalenko, V.I., Mongush, A.A., Ageeva, O.A., Fenshin, G., 2014. Sources and geodynamic environments of formation of Vendian–early Paleozoic magmatic complexes in the Dariv Range, Western Mongolia. Petrology 22 (4), 389–417.

Kozakov, I.K., Sal'nikova, E.B., Bibikova, E.V., Kirnozova, T.I., Kotov, A.B., Kovach, V.P., 1999. Polychronous evolution of the Paleozoic granitoid magmatism in the Tuva–Mongolia massif: U–Pb geochronological data. Petrologiya 7 (6), 631–643.

Kozakov, I.K., Sal'nikova, E.B., Khain, E.V., Kovach, V.P., Berezhnaya, N.G., Yakovleva, S.Z., Plotkina, Yu.V., 2002. Early Caledonian crystalline rocks of the Lake Zone in Mongolia: formation history and tectonic settings as deduced from U–Pb and Sm–Nd datings. Geotectonics 36 (2), 156–166.

Kozlovsky, A.M., Yarmolyuk, V.V., Salnikova, E.B., Travin, A.V., Kotov, A.B., Plotkina, J.V., Kudryashova, E.A., Savatenkov, V.M., 2015. Late Paleozoic anorogenic magmatism of the Gobi Altai (SW Mongolia): Tectonic position, geochronology and correlation with igneous activity of the Central Asian Orogenic Belt. J. Asian Earth Sci. 113 (1), 524–541.

Kröner, A., Kovach, V., Belousova, E., Hegner, E., Armstrong, R., Dolgopolova, A., Seltmann, R., Alexeiev, D.V., Hoffmann, J.E., Wong, J., Sun, M., Cai, K., Wang, T., Tong, Y., Wilde, S.A., Degtyarev, K.E., Rytsk, E., 2014. Reassessment of continental growth during the accretionary history of the Central Asian Orogenic Belt. Gondwana Res. 25, 103–125.

Kurenkov, S.A., Didenko, A.N., Simonov, V.A., 2002. Geodynamics of Paleospreading [in Russian]. GEOS, Moscow.

Kutolin, V.A. (Ed.), 1974. Tectonics of the Mongolian People's Republic [in Russian]. Nauka, Moscow.

Le Maitre, R.W.A., 1989. Classification of Igneous Rocks and Glossary of Terms: Recommendations of the International Union of Geological Sciences, Subcommission on the Systematics of Igneous Rocks. Blackwell, Oxford.

Ludwig, K.R., 1999. User's Manual for Isoplot/Ex, Version 2.10. A Geochronological Toolkit for Microsoft Excel. Berkeley Geochronol. Center Spec. Publ. 1a.

Ludwig, K.R., 2000. SQUID 1.00. A User's Manual. Berkley Geochronol. Center Spec. Publ. 2.

Maniar, P.D., Piccoli, P.M., 1989. Tectonic discrimination of granitoids. Geol. Soc. Am. Bull. 101, 635–643.

Mongush, A.A., Lebedev, V.I., Kovach, V.P., Sal'nikova, E.B., Druzhkova, E.K., Yakovleva, S.Z., Plotkina, Yu.V., Zagorskaya, N.Yu., Travin, A.V., Serov, P.A., 2011. The tectonomagmatic evolution of structure-lithologic complexes in the Tannu-Ola zone, Tuva, in the Late Vendian–Early Cambrian (from geochemical, Nd isotope, and geochronological data). Russian Geology and Geophysics (Geologiya i Geofizika) 52 (5), 503–516 (649–665).

O'Connor, J.T., 1965. A classification for quartz-rich igneous rocks based on feldspar ratios. U.S. Geol. Survey Prof. Paper 525B, B79–B84.

Rickwood, P.C., 1989. Boundary lines within petrologic diagrams which use oxides of major and minor elements. Lithos 22, 247–263.

Rudnev, S.N., 2013. Early Paleozoic Granitoid Magmatism of the Altai–Sayan Folded Area and Lake Zone in Western Mongolia [in Russian]. Izd. SO RAN, Novosibirsk.

Rudnev, S.N., Borisov, S.M., Babin, G.A., Levchenkov, O.A., Makeev, A.F., Serov, P.A., Matukov, D.I., Plotkina, Yu.V., 2008. Early Paleozoic batholiths in the northern part of the Kuznetsk Alatau: composition, age, and sources. Petrology 16 (4), 395–420.

Rudnev, S.N., Izokh, A.E., Kovach, V.P., Shelepaev, R.A., Terent'eva, L.B., 2009. Age, composition, sources, and geodynamic environments of the origin of granitoids in the northern part of the Ozernaya Zone, Western Mongolia: growth mechanisms of the Paleozoic continental crust. Petrology 17 (5), 439–475.

Rudnev, S.N., Izokh, A.E., Borisenko, A.S., Shelepaev, R.A., Orihashi, Y., Lobanov, K.V., Vishnevsky, A.V., 2012. Early Paleozoic magmatism in the Bumbat–Hairhan area of the Lake Zone in western Mongolia (geological, petrochemical, and geochronological data). Russian Geology and Geophysics (Geologiya i Geofizika) 53 (5), 425–441 (557–578).

Rudnev, S.N., Kovach, V.P., Ponomarchuk, V.A., 2013a. Vendian–Early Cambrian island-arc plagiogranitoid magmatism in the Altai–Sayan folded area and in the Lake Zone of western Mongolia (geochronological, geochemical, and isotope data). Russian Geology and Geophysics (Geologiya i Geofizika) 54 (10), 1272–1287 (1628–1647).

Rudnev, S.N., Babin, G.A., Kovach, V.P., Kiseleva, V.Yu., Serov, P.A., 2013b. The early stages of island-arc plagiogranitoid magmatism in Gornaya Shoriya and West Sayan. Russian Geology and Geophysics (Geologiya i Geofizika) 54 (1), 20–33 (27–44).

Rudnev, S.N., Serov, P.A., Kiseleva, V.Yu., 2015. Vendian–Early Paleozoic granitoid magmatism in Eastern Tuva. Russian Geology and Geophysics (Geologiya i Geofizika) 56 (9), 1232–1255 (1572–1600).

Rudnev, S.N., Izokh, A.E., Borisenko, A.S., Gas'kov, I.V., 2016. Granitoid magmatism and metallogeny of the Lake Zone in Western Mongolia (by the example of the Bumbat-Hairhan area). Russian Geology and Geophysics (Geologiya i Geofizika) 57 (2), 207–224 (207–224).

Rudnev, S.N., Mal'kovets, V.G., Belousova, E.A., Tret'yakova, I.G., Gibsher, A.A., 2018. U–Pb isotope dating of xenogenic zircon from

early Paleozoic plagiogranitoids of the southern part of the Lake Zone in Mongolia, in: Methods and Geological Results of Study of Geochronometric Isotope Systems of Minerals and Rocks. Proceedings of the Seventh Russian Conference on Isotope Geochronology [in Russian]. IGEM RAN, Moscow, pp. 294–297.

Terent'eva, L.B., Kozakov, I.K., Yarmolyuk, V.V., Anisimova, I.V., Kovach, V.P., Kozlovskii, A.M., Kudryashova, E.A., Sal'nikova, E.B., Yakovleva, S.Z., Fedoseenko, A.M., Plotkina, Yu.V., 2010. Convergent processes in the evolution of the early Caledonian Bayan-Khongor zone of Central Asia: Evidence from geological and geochronological investigations of the Khan-Ula gabbroid pluton. Dokl. Earth Sci. 433 (1), 937–943.

Togtoh, D., Baatarhuag, A., Gansuh, D., Ganzorig, D., Ganbaatar, G., Bayardalay, C., Usna-Ah, C., Anhbayar, B., Davaadorzhd, D., Gandesh, B., Anhzhin, C., 1993. Geological Survey of the Mongolian. Scale of 1 : 200,000 (Darvi, Tonhil, Tugrug–200). Geological Information Centre, MRPAM, Ulaanbaatar.

Tomurtogoo, O. (Ed.), 1999. Geological Map of Mongolia. General Directorate of Mineral Research and Exploration of Turkey, Ankara.

Wiedenbeck, M., Alle, P., Corfu, F., Griffin, W.L., Meier, M., Oberli, F., Vonquadt, A., Roddick, J.C., Speigel, W., 1995. Three natural zircon standards for U–Th–Pb, Lu–Hf, trace-element and REE analyses. Geostand. Newslett. 19, 1–23.

Williams, I.S., 1998. U–Th–Pb geochronology by ion microprobe, in: McKibben, M.A., Shanks, W.C., Ridley, W.I. (Eds.), Applications of Microanalytical Techniques to Understanding Mineralizing Processes. Rev. Econ. Geol. 7, 1–35.

Yarmolyuk, V.V., Kovalenko, V.I., Kovach, V.P., Kozakov, I.K., Kotov, A.B., Sal'nikova, E.B., 2002. Isotopic composition, sources of crustal magmatism, and crustal structure of Caledonides of the Ozernaya Zone, Central Asian Foldbelt. Dokl. Earth Sci. 387A (9), 1043–1047.

Yarmolyuk, V.V., Kovalenko, V.I., Kovach, V.P., Kozakov, I.K., Kotov, A.B., Sal'nikova, E.B., 2003. Geodynamics of Caledonides in the Central Asian Foldbelt. Dokl. Earth Sci. 389A (3), 311–316.

Yarmolyuk, V.V., Kovalenko, V.I., Kovach, V.P., Rytsk, E.Yu., Kozakov, I.K., Kotov, A.B., Sal'nikova, E.B., 2006. Early stages of the Paleoasian Ocean formation: Results of geochronological, isotopic, and geochemical investigations of Late Riphean and Vendian-Cambrian complexes in the Central Asian Foldbelt. Dokl. Earth Sci. 411 (1), 1184–1189.

Yarmolyuk, V.V., Kovach, V.P., Kovalenko, V.I., Salnikova, E.B., Kozlovskii, A.M., Kotov, A.B., Yakovleva, S.Z., Fedoseenko, A.M., 2011. Composition, sources, and mechanism of continental crust growth in the Lake Zone of the Central Asian Caledonides: I. Geological and geochronological data. Petrology 19 (1), 55–78.

Editorial responsibility: A.E. Izokh